University of Pretoria etd

Chapter 3
MODELLING OF THE ELECTRICALLY STIMULATED COCHLEA

Some of the results in this chapter have been accepted for publication in *Ear and Hearing* under the title "Three-dimensional spiraling finite element model of the electrically stimulated cochlea".

1 INTRODUCTION

The pitch sensation created during intracochlear stimulation is a function of place of stimulation and frequency of stimulation (Clark, 1996), but could also be a function of the physical placement of individual electrode contacts relative to the surviving nerve fibres, the geometry of the electrode contacts and the anatomy of the cochlea (Fu & Shannon, 1999a, 1999b; Rebscher et al., 1996; Shannon, 1983). In this chapter the effect of the placement and geometry of electrode contacts on excitation patterns for a specific cochlear geometry is considered. The shape of potential distributions around intracochlear electrodes could determine the characteristics of the place pitch information that can be provided with a specific implant system. More localized potential distributions and thus excitation patterns provide more degrees of freedom to shape the excitation pattern of the auditory nerve (Liang, Lusted, & White, 1999). An analysis of information supplied by stimulation with various electrode configurations is presented. In addition, the effect of the anatomical detail of the model is investigated to provide a qualitative indication of the degree of detail that is required in volume conduction models of the implanted cochlea.

University of Pretoria etd

2 MODEL AND METHODS

The combined FE-nerve fibre model described in Chapter 2 was used to investigate the effect of the electrode configuration, including electrode geometry and array location and parameter variations in the FE model, on the potential distributions and neural excitation patterns around intracochlear electrodes.

The most important output from the FE model is the shape (and not the absolute value) of the potential distribution (Rodenhiser & Spelman, 1995), as long as the intensity of the potential distribution is adequate to elicit a response. This is mainly because nerve fibre activation patterns are directly related to the shape and size (i.e. the spread) of the potential distributions. This relationship is described by the activating function (Rattay, 1999) that expresses the excitability of a nerve fibre as a function of the second spatial derivative of the electrical potential field along the length of the nerve fibre.

2.1 Electrode configuration and geometry

In this section variations in electrode configuration and geometry, and array location (hereafter collectively called "array variations") are discussed.

2.1.1 Longitudinal electrode configurations

Eight different longitudinal electrode configurations were modelled: narrow bipolar (NBP)[1], bipolar (BP), BP+1, BP+2, BP+3, two pseudo-monopolar or apical reference (AR1 and AR2)[2] configurations (Fig 3.1a) and one true monopolar configuration (MONO). For the true monopolar configuration the outer boundaries of the FE model

[1]NBP mode refers to an electrode spacing approximately half of the spacing between adjacent electrodes in the Nucleus cochlear implant (Clark, 1996).

[2]Pseudo-monopolar mode is not a true monopolar mode, as the reference is not located remotely, but inside the scala. This mode will be called "apical reference" (AR) mode.

University of Pretoria etd

(i.e. the external surfaces of the bone cylinder) were defined as an equipotential surface serving as the return electrode.

Table 3.1. Electrode dimension details of longitudinal electrode configurations.

[a] The interelectrode spacing is dependent on the exact location in the model. At this specific location in the model the interelectrode spacing is 828 m.

[b] The interelectrode spacing is taken as the length of the straight line crossing through the modiolus and connecting the centre of the electrode carrier between segments 19 and 55.

[c] The interelectrode spacing is taken as the length of the straight line connecting the centre of the electrode carrier between segments 19 and 80.

Electrode configuration	**Model segment number used as electrode**		**Inter-electrode spacing m**		
	basal	**apical**	**Nucleus**	**Lateral**	**Medial**
near BP	19	21	n.a.	277	277
BP	19	23	700	828[a]	688
BP + 1	19	26	1 700	1 646	1 365
BP + 2	19	30	2 700	2 719	2 252
BP + 3	19	34	3 700	3 775	3 121
AR1[b]	19	55	n.a.	7 944	6 685
AR2[c]	19	80	n.a.	1 665	1 468

AR1 electrode configurations were modelled because many subjects using the Nucleus implant have not been fitted with an extracochlear return electrode. However, pshychoacoustic data are available for AR1 electrode configuration for subjects wearing the Nucleus implant (Hanekom & Shannon, 1998). Also, since the electrode separation in AR1 electrode configuration is large, the effect of one electrode on the potential field at the nerve fibers close to the other electrode is small (less than 1% if a medium with uniform resistivity is assumed and potential field decay is assumed to be inversely proportional to distance). Each electrode in the

University of Pretoria etd

AR1 pair could thus be viewed as approximating a monopole, i.e., an AR1 electrode configuration approximates a "double" monopolar electrode configuration. The neural excitation pattern around any one of the electrodes in an AR1 configuration could thus be expected to be similar to that around a true monopolar electrode.

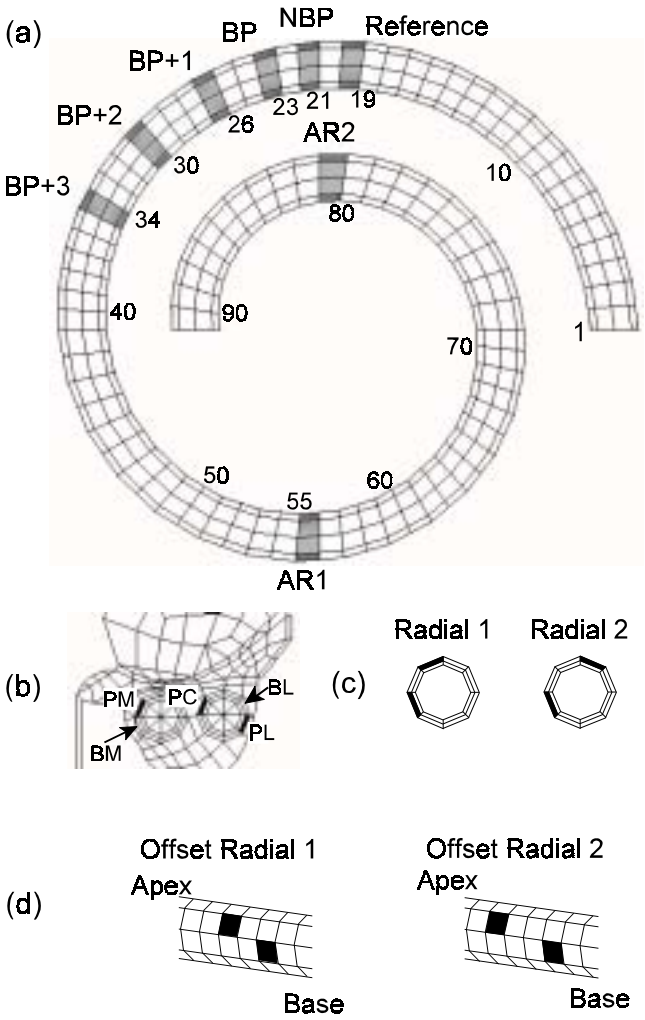

Figure 3.1. (a) Locations of electrode contacts along the length of the electrode carrier for longitudinal banded and longitudinal point configurations. Locations of electrode contacts on the perimeter of the electrode carrier for (b) longitudinal point (PM, PC and PL), (c) radial and (d) offset radial configurations. The locations of the BM and BL arrays can also be seen on (b).

University of Pretoria etd

AR2 electrode configurations were modelled to study the effect of electrodes that are placed in neighbouring canals.

Two banded array locations are modelled: one in a medial location in the scala tympani close to the modiolus (called "banded medial" or "BM") and one in a location lateral to the close to the outer wall of the scala tympani (called "banded lateral" or "BL"). Figure 3.1 shows the location of the two array locations. Point electrodes were modelled at three locations, medial, central and lateral in the scala tympani (called "PM", "PC" and "PL" respectively) and are shown in Figure 3.1b. Table 3.1 summarizes the details of the longitudinal electrode configurations. Electrode carrier diameters are 0.5 mm for banded electrode configurations and 0.6 mm for point electrode configurations.

2.1.2 Radial electrode configurations

Radial or offset radial electrode configurations are used in some implants, for example the Clarion implant from Advanced Bionics Corporation (Kessler, 1999). Narrowly spaced and widely spaced radial (Figure 3.1c) and offset radial configurations (Figure 3.1d) were modelled. The basal electrode in the offset radial configurations is inferior relative to the apical electrode. Dimensional details of the radial electrode configurations are given in Table 3.2. The carrier diameter is 0.6 mm.

Table 3.2. Electrode dimension details of radial electrode configurations.

Electrode configuration	**Model segment number used as electrode**		**Inter-electrode spacing (m)**
	return	**active**	
R1	19	19	392
R2	19	19	589
OR1	19	20	688
OR2	19	21	1 000

University of Pretoria etd

2.1.3 Hifocus-like[3] electrode geometry

The Hifocus electrode (Advanced Bionics Corporation, 2000) was designed to deliver highly selective electrical stimulation to the auditory nerve fibres and to limit channel interaction by limiting longitudinal current flow. The array is designed to assume a perimodiolar position and thus target the spiral ganglion cells for stimulation. This electrode is suitable for simultaneous stimulation on more than one electrode pair (or channel) because of the inhibition of lateral current flow.

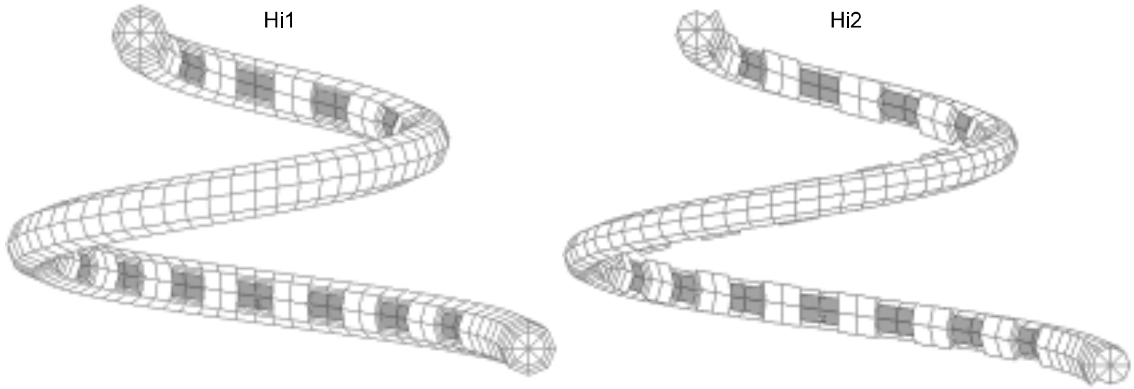

Figure 3.2. Two modelled Hifocus-like electrode arrays. The left array (Hi1) has its contacts recessed into the electrode carrier, while the right array (Hi2) has pillows of insulating material between the contacts.

Table 3.3. Electrode dimension details of Hifocus-like electrode array.

Electrode configuration	**Model segment numbers used as electrode**		**Approximate inter-electrode spacing in mm (centre to centre)**
	basal	**apical**	
BP	8-9	12-13	1.0
BP+1	8-9	16-17	1.9
AR1	12-13	55-56	6.9

[3]The Hifocus electrode is a new electrode design that creates highly focussed electrical stimulation (Advanced Bionics Corporation, 2000).

University of Pretoria etd

Two approximations of the Hifocus electrode were modelled. The first model (called Hi1 hereafter) was constructed by recessing the electrode contacts into the insulating electrode carrier. This configuration is shown in the left part of Figure 3.2. The second model (called Hi2 hereafter) was constructed by placing pillows of an insulating material (the same material as the electrode carrier for these simulations) between the contacts. The Hi2 FE model is shown in the right part of Figure 3.2. The surface area of the contacts was approximately 0.25 mm^2 but varied slightly as a function of location in the model (Figure 2.7). Recess depth (Hi1) and the height of the interelectrode pillows (Hi2) were 100 m.

2.2 Model parameter variations

2.2.1 Tapering of the scala tympani

To simulate tapering of the cochlea towards the apex, the resistivity of the perilymph was scaled to render lower resistivity in the basal region of the cochlea and higher resistivity towards the apex. Lower resistivity simulates a wider canal while higher resistivity simulates a narrower canal. The upper graph in Figure 3.3 shows the width of the scala tympani as a function of position along the length of the scala tympani. The percentage error between the width in the modelled scala tympani and the measured widths is also shown.

To determine a scaling function for the resistivity, a second order polynomial was fitted to the error function. Scaled resistivities $_{new}$ were determined by the equation

$$\rho_{new} = \frac{\rho_{model}}{1 + e} \tag{3.1}$$

where $_{model}$ = 700 -mm and is the error expressed as a fraction.

The resistivities were averaged over six FE model sections to render the discretized resistivity function shown in the lower part of Figure 3.3. The primary objective of the discretization was to reduce the number of sections for which the resistivities had to be changed from 90 sections to 15 sections. The polynomial fit was preferred above

University of Pretoria etd

a fit to the measured data because it produced smaller discontinuities between neighbouring model sections.

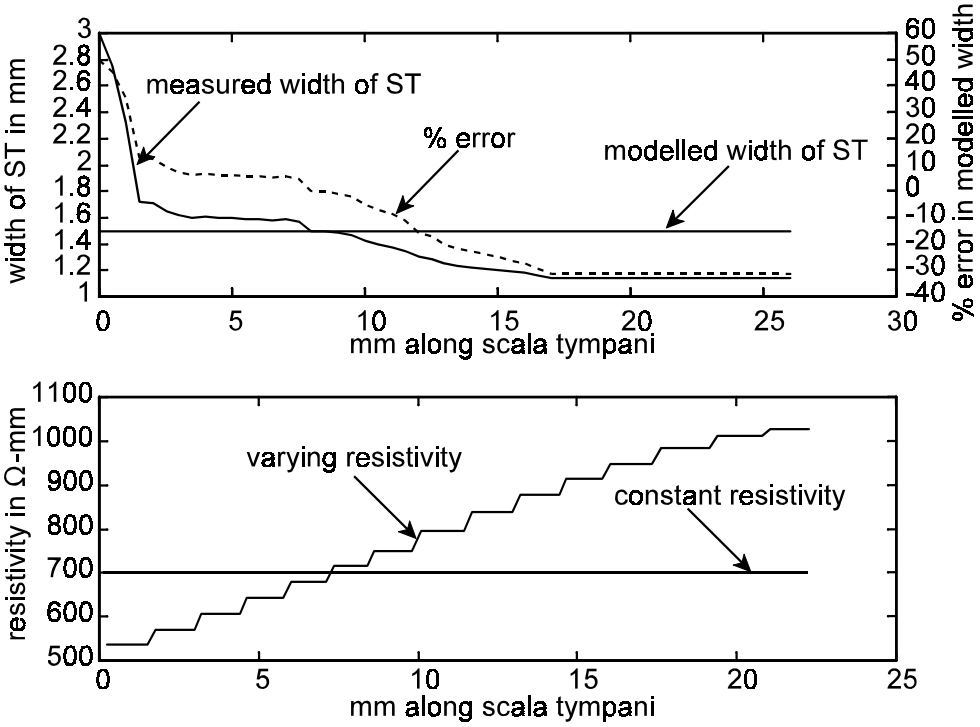

Figure 3.3. The upper graph shows the measured width of the human scala tympani (Hatsushika et al., 1990), the (constant) modelled width and the percentage error between the real and modelled widths as a function of distance along the scala tympani. The lower graph shows the varying perilymphatic resistivity that was used to simulate tapering of the cochlea and also the constant resistivity when no tapering was simulated.

2.2.2 Helicotrema

The effect of the connection between the scala tympani and the scala vestibuli on excitation patterns was investigated by changing the material properties of the last section of the scala media and surrounding membranes in the FE model to that of perilymph. This simulates a conductive pathway from the scala tympani to the scala vestibuli. Neural excitation patterns were determined for electrode locations close to the "helicotrema" and also for electrode locations in the first half-turn of the model (corresponding to the locations in Figure 3.1).

University of Pretoria etd

2.2.3 Other modelled structures

The effect of the fine structure of the cochlea on potential distributions and a qualitative indication of the sensitivity of model results to these structures were determined by merging the structure under investigation into the structure in contact with it. Details of structures that were investigated are given in Table 3.4.

Table 3.4. Details of structural changes to the FE model. The resistivity of the applicable structure is changed to that of the surrounding tissues.

Structure	Description	Correct -mm	New -mm
Organ of Corti	Organ of Corti is merged into scala media.	83 333	600
Stria vascularis	Stria vascularis is merged into bone.	125 790	6 410
Reissner's membrane	Reissner's membrane is merged into scala vestibuli.	340 130	700
Spiral lamina	Spiral lamina is merged into scalae tympani and vestibuli.	6 410	700
Basilar membrane	Basilar membrane is merged into scalae tympani and vestibuli.	4 000	700

2.3 Modelling of auditory nerve excitation

In this study the focus was not on the exact location of the site of excitation along the length of a nerve fibre, but rather on whether a particular nerve fibre is activated or not. A propagating action potential was assumed to signify neural excitation (Reilly, Freeman, & Larkin, 1985). Threshold currents were determined by examining the 16^{th} node of each nerve fibre for the occurrence of an action potential. The occurrence of an action potential was detected by an iterative process. An interval was defined in which the threshold current was expected to occur. The current level was then stepped down or up by halving the interval with each iteration depending

University of Pretoria etd

on whether the current level caused an action potential or not. The final resolution of the iterative process was 1 A.

The stimulation waveform used was a single balanced phase square pulse with cathodic and anodic phases equal to 0.2 ms. The more apical electrode was used to deliver the cathodic-first stimulus, unless otherwise noted. Neural responses were calculated over a period of 1 ms.

3 RESULTS

3.1 Potential distributions and AF contours

Potential distributions and AF contours are presented in this section. The activating function is calculated along the length of a single nerve fibre and gives an indication of the exciting ability (a positive value for the activating function indicates possible excitation) of the extracelluler potential distribution (i.e. the potential distribution as a result of stimulation). An AF contour plot is a two-dimensional graph showing the intensity of the activating function over all modelled nerve fibres. Maxima and minima in this AF contour plot give a relative indication of the spread of neural excitation without calculating the neural response with a nerve fibre model. Potential distributions and AF contours are discussed in three categories. First, an overview is given of occurrences that are common to all array locations, electrode configurations and electrode geometries. Secondly, potential distributions as a result of specific model structure and parameter variations are discussed. Only selected variations in model structure and parameters are discussed since not all variations render clearly visible differences in the potential distributions. Lastly, potential distributions and AF contours generated with Hifocus-like electrode geometries are presented.

3.1.1 Overview

A 200 A dc stimulation current was used to calculate potential distributions.

University of Pretoria etd

Although potential distributions were calculated with a dc stimulus, biphasic stimuli could be generated by scaling because of the resistive nature of the FE model. Potential distributions were calculated on the nerve fibres in the FE model.

Figure 3.4 shows potential distributions (left) and AF contours (right) for BP and BP+3 configurations for the PM (upper four graphs) and BL (lower four graphs) arrays calculated with the FE model. Figure 3.5 shows potential distributions for similar electrode configurations for medial (upper four graphs) and lateral (lower four graphs) array locations calculated with the analytical model. In Figure 3.4 equipotential lines are for 20 mV increments for the PM array and for 10 mV increments for the BL array. Equipotential lines are alternately labelled (except for the additional 0 V label on the plots for the PM array). No absolute values for potentials or activating function intensity are given for the analytically calculated contours (Figure 3.5) since only qualitative comparison between FE calculated and analytically calculated potential distributions is possible, i.e. the shapes and relative intensities of the potentials and AF contours calculated with the analytical model are compared to results obtained with the FE model. Vertical dashed lines indicate boundaries between the half-turns of the modelled cochlea while vertical solid lines indicate the location of the electrodes along the length of the basilar membrane.

Potential distributions for different electrode locations and geometries are similar for different electrode separations, i.e. maxima and minima are located at approximately the same distance along the nerve fibres relative to the fibre terminals, but at different locations along the basilar membrane, depending on the location of the electrode contacts. The intensity of the potential field is, however, higher for widely spaced electrode configurations than for narrowly spaced configurations (compare potential maxima and minima for BP and BP+3 electrode configurations). This is because the impedance between the electrode contacts (and thus over the tissues between the electrode contacts) increases, causing an increase in the voltage drop between the electrode contacts.

University of Pretoria etd

Since the BL array is more distally located from the nerve terminals than the PM array, the location of the maximum potential along the length of the nerve fibres is displaced. This is also visible in results from the analytical model. Maxima and minima in the potential distribution on the nerve fibres occur at the point where the nerve fibres are closest to the electrode contacts.

Potential maxima and minima differ substantially between banded electrode geometries (lower part of Figure 3.4) and point electrode geometries (upper part of Figure 3.4) using the same stimulus intensity. Furthermore, potential fields are narrowest for closely spaced electrode configurations and increase with increasing interelectrode separation. This can be seen both in results from the FE model and from the analytical model when potential distributions for BP and BP+3 electrode configurations are compared. The spread of excitation is also expected to increase for more widely spaced electrode configurations because of the wider spread of the maxima and minima in the AF contours relative to maxima and minima in the same plots for narrowly spaced electrode configurations.

Contrary to the analytical model, potential distributions generated with the FE model (Figure 3.4) are not symmetrical because of the spiralling nature of the cochlea. A toroidal model generated from the same 2-D geometry from which the spiralling model was created (Figure 2.4) produced symmetric potential distributions. The results of the toroidal model are not shown. The width[4] of potential distributions is a function of both array location and electrode configuration. NBP electrode configurations create wider potential distributions in the region of the more *apical* electrode for all array locations, while wider electrode separations usually create

[4]The width of the potential field refers to distance from the electrode where a specific magnitude of potential occurs, i.e. a 10 mV potential magnitude will occur further away from the electrode for a wide potential distribution than for a narrow potential distribution. The width is qualitatively evaluated on a line parallel to the basilar membrane on the neural plane at the location of the electrodes, i.e., the "0 mm along nerve fiber" line for lateral electrode arrays and approximately the "0.5 mm along nerve fiber"-line for medial electrodes.

University of Pretoria etd

wider potential distributions around the more *basal* electrode. The electrode separation where the transition occurs from wider distributions around the more apical electrode to wider distributions around the more basal electrode is a function of the array location. Array locations closer to the nerve fibres often create wider potential distributions around the *basal* electrode than array locations further away from the nerve fibres.

For array locations close to the nerve fibres and the fibre terminals (i.e. BM, BL, PM and PC) the transition occurs at BP+1 electrode configuration and at BP+2 electrode configuration for the PL array. This could, however, partly be a result of the slightly larger surface area of the model segments toward the basal end of each half-turn. The effect of variation in electrode surface area is expected to be greater for electrode arrays close to the nerve fibres.

AF contours for potential distributions generated with the FE model show locations of possible ectopic stimulation (i.e. stimulation of nerve fibres other than the target nerve fibres) in the third half-turn of the modelled cochlea. Since the intensity of the AF contour plot at this location in the model is low compared to its intensity in the first half-turn, excitation thresholds can be expected to be higher. The intensity of the AF contours at the ectopic location shows that ectopic excitation can be expected to occur at lower stimulation currents for array locations close to the nerve fibres (i.e. the BM array) and for widely spaced electrode configurations (BP+3 in the case shown). The analytical model does not show this ectopic region of excitation.

University of Pretoria etd

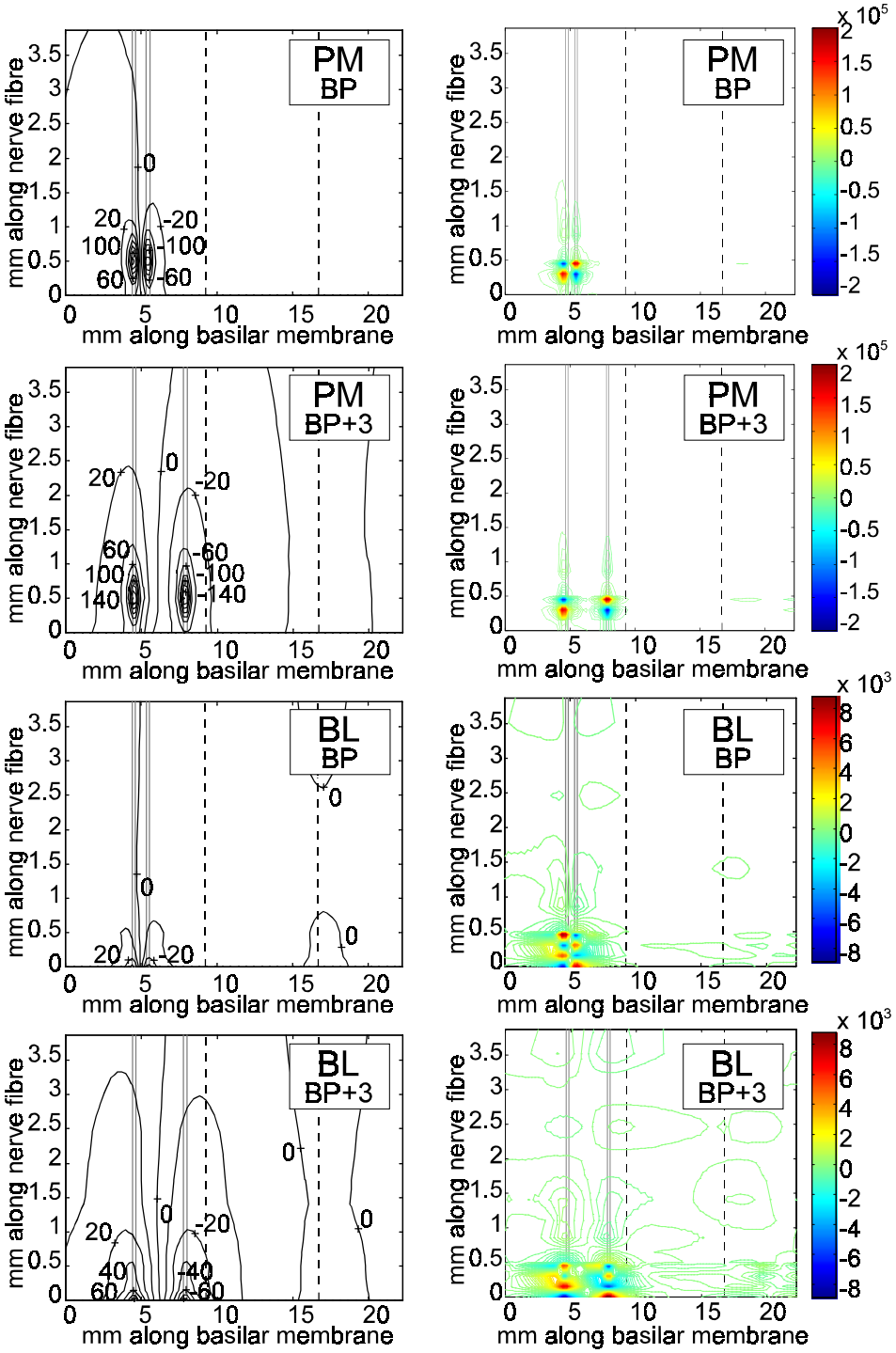

Figure 3.4. Potential distributions (left) and AF contours (right) for the BP and BP+3 electrode configurations for the PM array (upper four graphs) and the BL array (lower four graphs) calculated with the FE model described in Chapter 2. Equipotential lines are for 10 mV intervals and are alternately labelled. Units of AF contours: mV/ms.

University of Pretoria etd

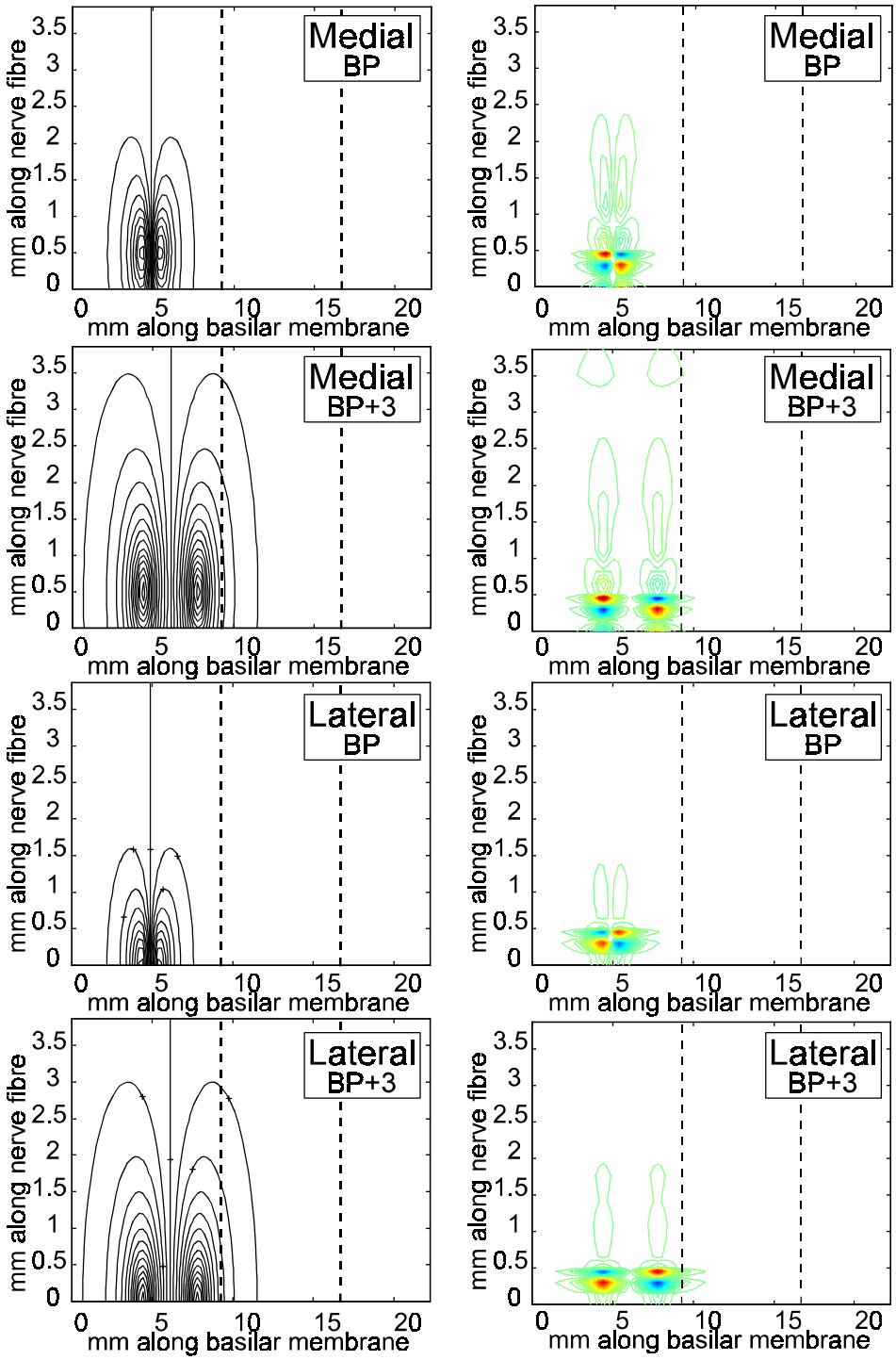

Figure 3.5. Potential distributions (left) and AF contours (right) for the BP and BP+3 electrode configurations for a medial array (upper four graphs) and a lateral array (lower four graphs) calculated with the analytical model described in Chapter 2.

University of Pretoria etd

3.1.2 Effect of model variations on potential distributions

3.1.2.1 Potential distributions with varying perilymphatic resistivity

Potential distributions increase in width from base to apex when the resistivity of the perilymphatic spaces is scaled to simulate tapering of the cochlea (left graphs in Figure 3.6). At the base, potential distributions are somewhat narrower for the scaled resistivity compared to the constant resistivity (upper two graphs in Figure 3.6). At the apex the situation is reversed (lower two graphs in Figure 3.6). Halfway through the first half-turn of the modelled cochlea the resistivities in the scaled and constant versions of the model were approximately equal. Consequently, potential distributions for the scaled and constant resistivities are approximately the same at this location (middle two graphs in Figure 3.6).

3.1.3 Hifocus-like electrode arrays

Figure 3.7 shows potential distributions (left graphs) and AF contours (right graphs) for the two Hifocus-like electrode geometries and a control geometry. The intensity of the potential field is higher for Hi1 (upper left) than for Hi2 (middle left) and the control geometry (lower left). Hi1 can be expected to have lower threshold currents because activating function intensity is higher than for Hi2 and the control electrode geometry. Potential distributions are similar for Hi2 and the control geometry except that distributions appear slightly elongated toward the medial processes of the nerve fibres for Hi2.

3.2 Auditory Nerve Excitation Patterns

Auditory nerve excitation patterns are characterized by calculating minimum threshold current (i.e. the current required to activate a single nerve fibre in the model) and by electrical tuning curves. The minimum threshold current gives an indication of the effectiveness of stimulation while electrical tuning curves show the localization of neural excitation.

University of Pretoria etd

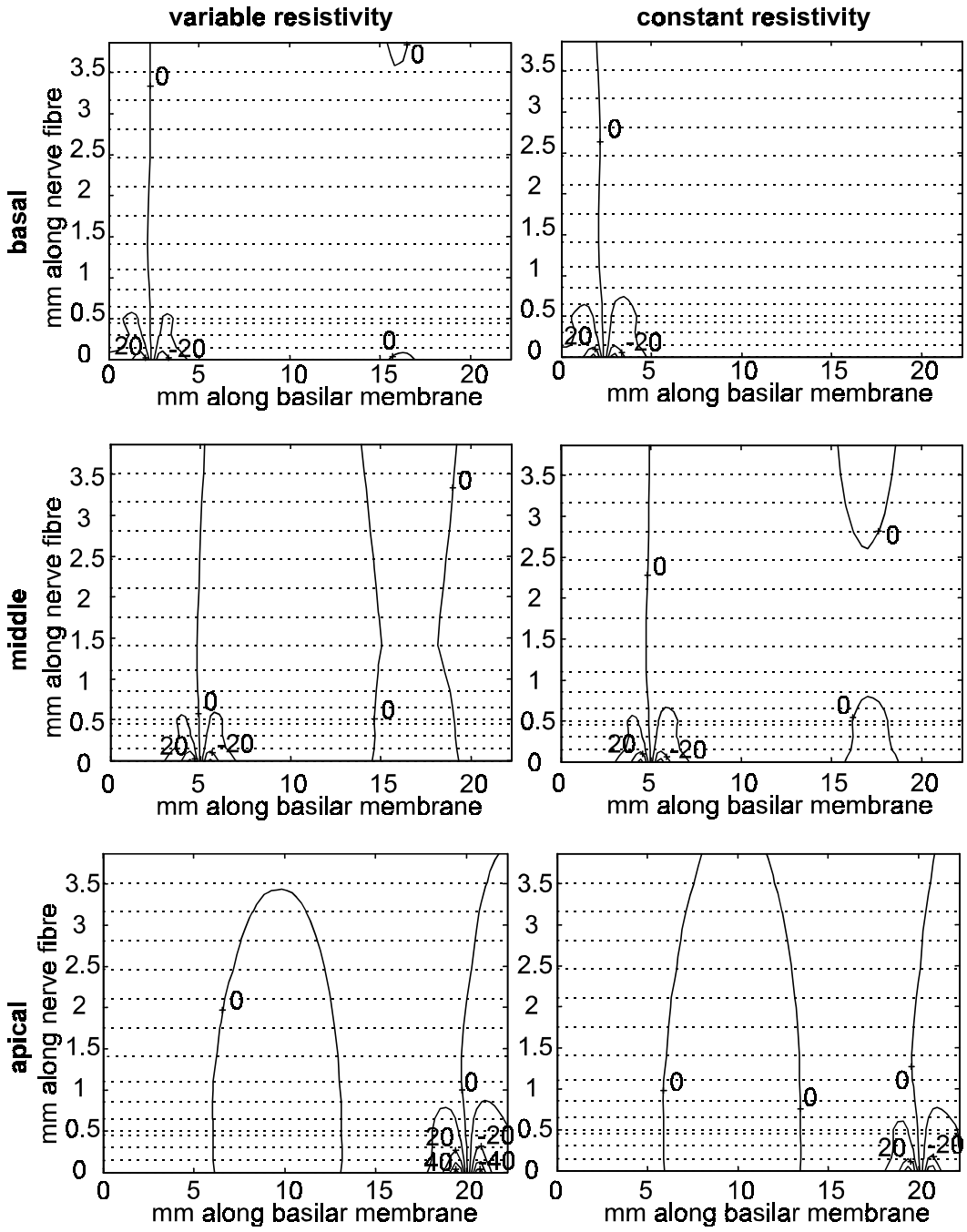

Figure 3.6. Potential distributions as a result of stimulation at different locations along the length of the basilar membrane. The graphs on the left are for an increase in the resistivity of the perilymph toward the apex, while the graphs on the right are for constant perilymphatic resistivity. Results are for the BL array. Equipotential lines are for 10 mV intervals and are alternately labelled.

University of Pretoria etd

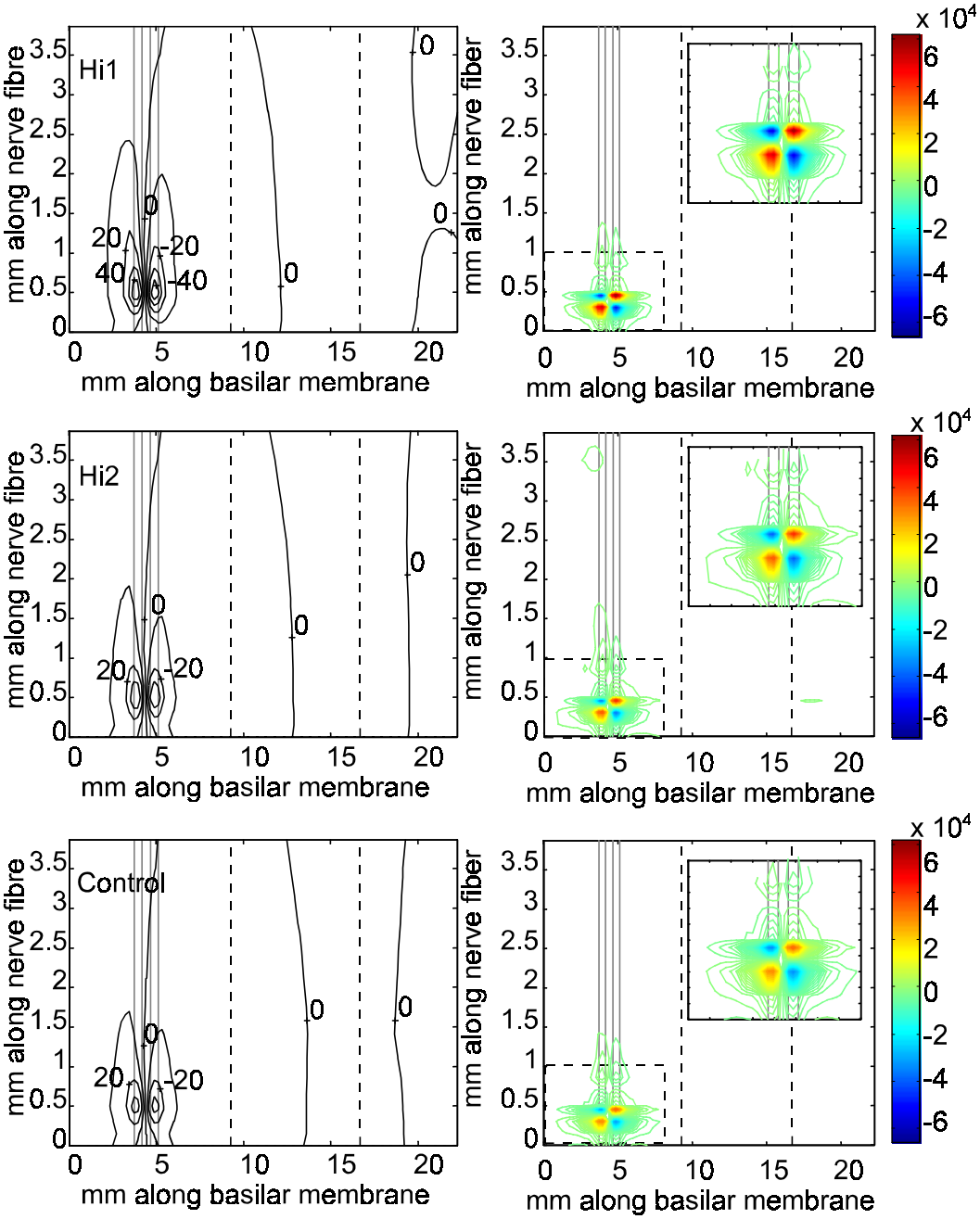

Figure 3.7. The graphs on the left show the potential distributions for BP electrode configuration created with Hi1 (upper), Hi2 (middle) and an unfocussed control geometry (lower), while the graphs on the right show AF contours for the same geometries (insets show an enlargement of the regions in dashed blocks). Equipotential lines (left graphs) are shown for 10 mV intervals and are alternately labelled. Units of AF contours: mV/ms.

University of Pretoria etd

3.2.1 Minimum threshold current

3.2.1.1 General trends

Figure 3.8 shows minimum threshold current versus electrode separation curves for both electrodes in a bipolar electrode pair. Minimum threshold current for anodic-first stimulation is defined as the lowest threshold for any nerve fibre close to the electrode delivering the anodic-first stimulus, while the opposite is true for cathodic-first minimum threshold current. Threshold currents were determined for full (intact) nerve fibres (16 nodes) as well as for truncated nerve fibres of which the peripheral axonal processes were degenerated (12 nodes). Results discussed are for the full nerve fibre model unless stated otherwise. Minimum threshold currents for cathodic-first stimulation are shown for monopolar stimulation for the full and truncated nerve fibre models (stars in Figure 3.8).

For longitudinal electrode configurations the model does not always predict the lowest threshold currents for nerve fibres close to the electrode delivering the cathodic-first stimulus (Figure 3.8). Threshold currents are always lower for nerve fibres around the *basal* electrode for closely spaced electrode configurations (NBP and BP). For more widely spaced configurations (BP+1 and wider), threshold currents are lower for nerve fibres around the cathodic-first electrode if the array overlaps with the nerve fibres. However, excitation also occurs on nerve fibres close to the cathodic-first electrode for array locations far from the fibres and widely spaced electrode configurations (AR1 and AR2) when a truncated nerve fibre model is used. Figure 3.9 show that anodic-first to cathodic-first threshold ratios are very close to unity. The greatest deviations from unity generally occur for closely spaced electrode configurations close to the nerve fibres. The dotted lines in Figure 3.8 show threshold currents for reversed stimulus polarity.

University of Pretoria etd

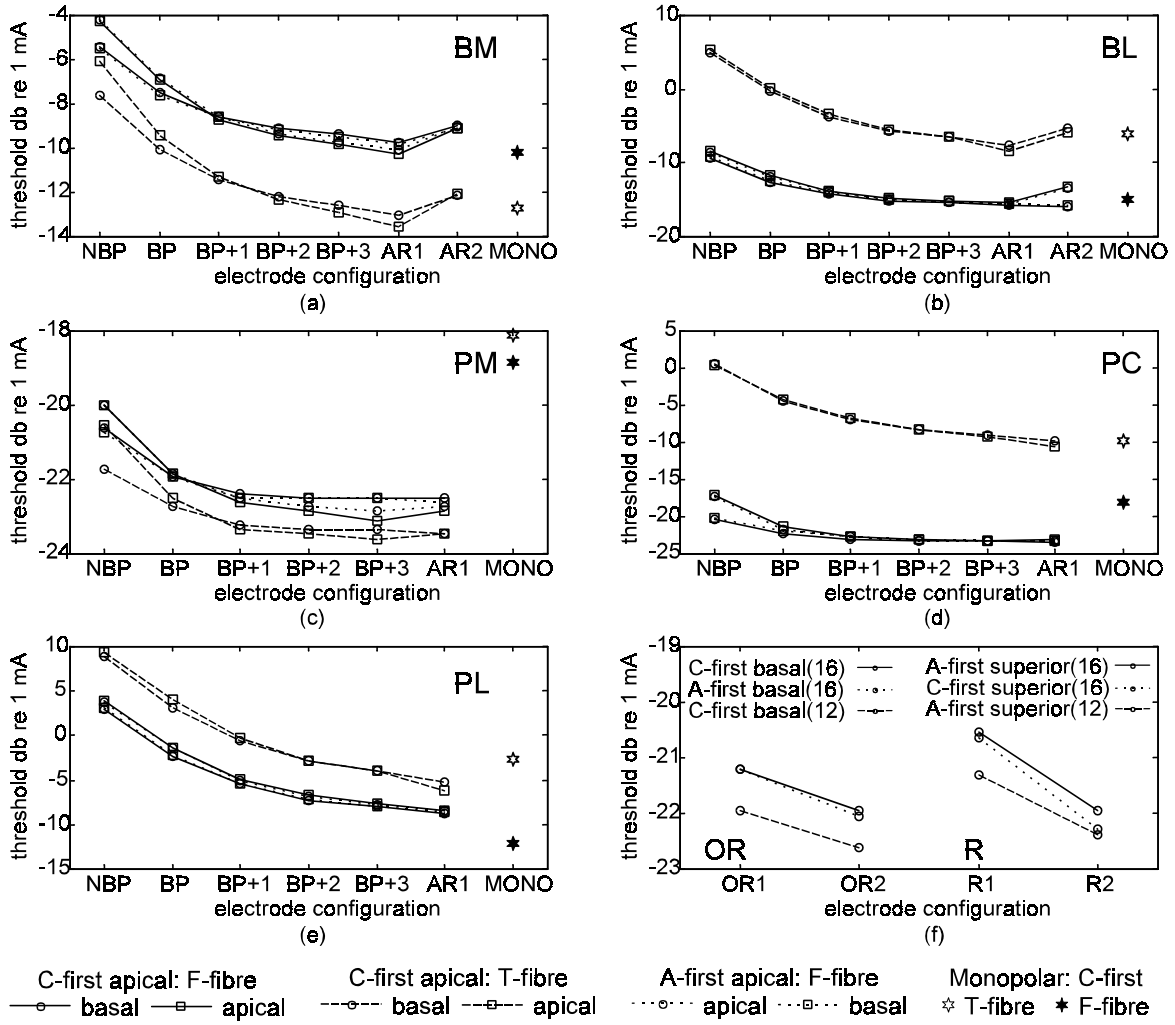

Figure 3.8. Threshold currents for nerve fibres activated by the electrode delivering the cathodic-first (Q) (C-first) and anodic-first (") (A-first) stimuli. Results are presented for both cathodic-first on the apical electrode (solid lines) and cathodic-first on the basal electrode (dotted lines) when a full nerve model is used, and for cathodic-first stimulation on the apical electrode when a truncated nerve model is used (dashed lines). (a) to (e) are results for longitudinal electrode configurations for the BM, BL, PM, PC, and PL arrays respectively, while (f) shows results for radial and offset radial electrode configurations. Threshold currents for cathodic-first monopolar stimulation are indicated with stars. The legend for figures (a) to (e) is at the lower edge of the figure. "F-fibre" is used to indicate the full nerve fibre model with 16 nodes and "T-fibre" to indicate the truncated nerve fibre model with 12 nodes.

University of Pretoria etd

When the polarity of the stimulation current is reversed, the model usually predicts minimum threshold currents to occur for the same nerve fibre. Thus, stimulus polarity does not influence the location of excitation along the basilar membrane. Also, the threshold current versus electrode separation curve for a specific electrode remains almost unchanged irrespective of stimulus polarity. Threshold currents are usually the lowest when the apical electrode in a bipolar pair delivers the cathodic-first stimulation, although this minimum current might excite nerve fibres close to the basal electrode. Typically, the model predicts lower threshold currents for nerve fibres near the basal electrode irrespective of stimulus polarity.

Similar to bipolar stimulation, threshold currents for monopolar stimulation are a function of array to surviving nerve fibre proximity and of electrode geometry. Generally, threshold currents are approximately the same as those for widely spaced bipolar electrode configurations. The exception is the PM and PC arrays where thresholds are substantially elevated from those of widely spaced bipolar configurations. This elevation in threshold current is most likely as a result of the configuration of the remote electrode. For monopolar stimulation the remote electrode is configured as an equipotential surface carrying a uniform current density over the outer boundaries of the bone cylinder. This causes current to be dispersed radially from the electrode contact, whereas current is directed mostly between the two electrodes in an AR configuration. Because of elevated threshold currents for the PM array, less variation exists between threshold currents for different electrode geometries and array locations for monopolar electrode configuration than for AR1 stimulation.

Truncation of the nerve fibre model causes minimum threshold currents to decrease for medial array locations (BM and PM) and to increase for lateral array locations (BL, PC and PL). The largest differences in threshold current are seen for the BL and PC arrays (approximately 7 dB to 15 dB) while the PM and BM arrays show the smallest differences (approximately 1 dB to 3 dB). The PL array is moderately influenced by nerve truncation with a threshold increase from the full to the truncated model of

University of Pretoria etd

approximately 6 dB. Figure 3.8f shows that threshold currents for pure radial and offset radial electrode configurations are comparable to threshold currents for bipolar stimulation with the PM array. Similar to longitudinal electrode configurations, threshold currents for radial and offset radial configurations are lower for widely spaced electrode pairs than for closely spaced electrode pairs. Lower threshold currents are achieved when the superior electrode is used to deliver the cathodic-first stimulus.

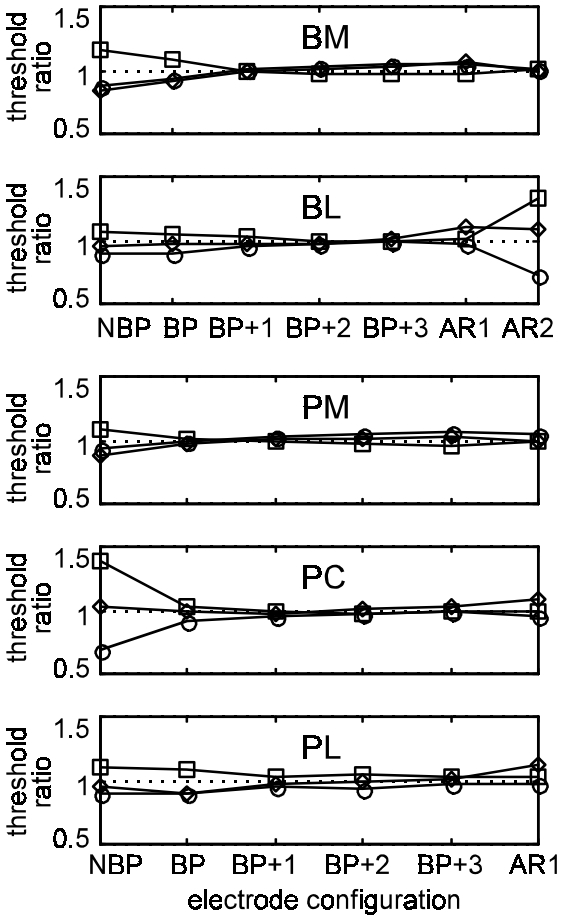

Figure 3.9. Anodic-first to cathodic-first threshold ratios for the BM, BL, PM, PC, and PL arrays as a function of electrode separation.

University of Pretoria etd

3.2.1.2 Threshold currents in a model with varying perilymphatic resistivity

The effect of varying the resistivity of the perilymphatic spaces in the modelled cochlea is to elevate threshold currents in the basal region while lowering these currents in the apical region of the model (Figure 3.10). Threshold currents for constant perilymphatic resistivity are relatively constant over the entire length of the modelled cochlea.

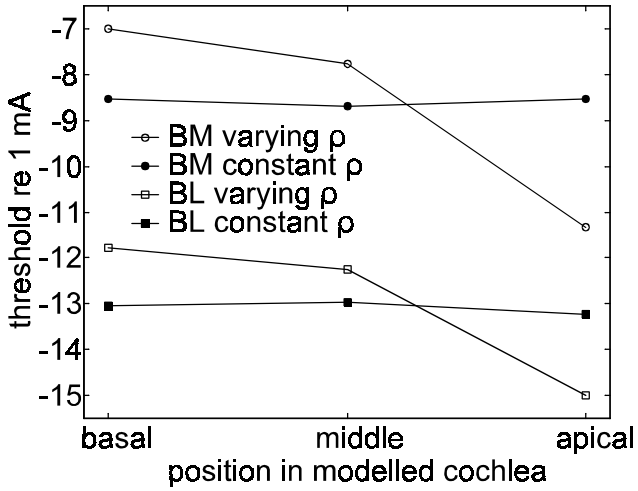

Figure 3.10. Threshold currents as a function of location in the modelled cochlea for constant and varying perilymphatic resistivities.

3.2.1.3 *Threshold currents for a Hifocus-like electrode geometry*

Minimum threshold current is lowest for the Hi1 geometry while the control geometry exhibits the highest minimum threshold current (Figure 3.11). Similar to banded and point electrode geometries, minimum threshold current is lower for widely spaced electrode configurations (AR1) than for narrowly spaced configurations (BP). Note that threshold currents are higher than those for the PM array because the surface area of the electrodes used for the Hifocus-like electrode geometries are approximately four times larger than the surface area of the electrodes used for the PM array.

University of Pretoria etd

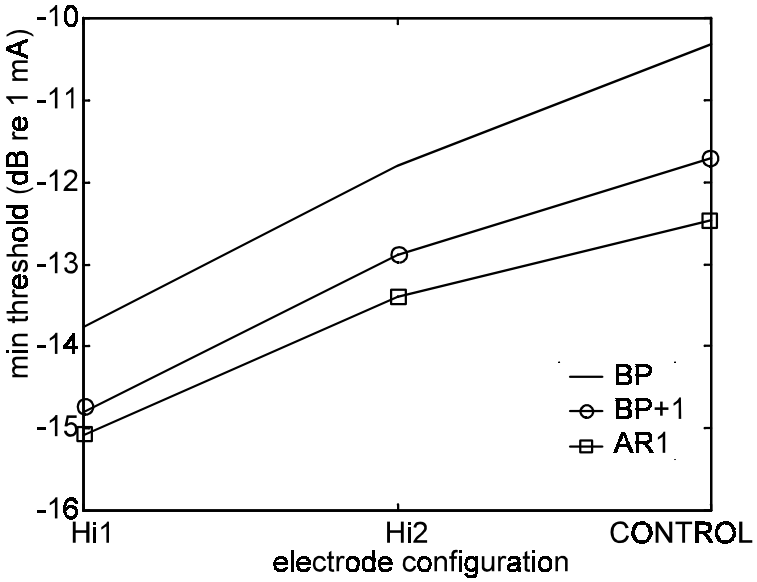

Figure 3.11. Minimum threshold current as a function of electrode geometry for BP, BP+1 and AR1 electrode configurations.

3.2.1.4 Influence of cochlear structures on minimum threshold currents

No discernable changes in threshold currents are observed when the helicotrema is simulated at the apical end of the FE model (results are thus not graphically presented). The cochlear structures that have the largest effect on threshold currents predicted with the model compared to other structures, are Reissner's membrane and the spiral lamina (Figure 3.12). The basilar membrane is the third most important structure, while the effects of the Organ of Corti and the stria vascularis are almost negligible. The influence of the basilar membrane might be more pronounced for array locations distal from the nerve fibres, i.e. the BL array, where the array is located directly next to the basilar membrane.

University of Pretoria etd

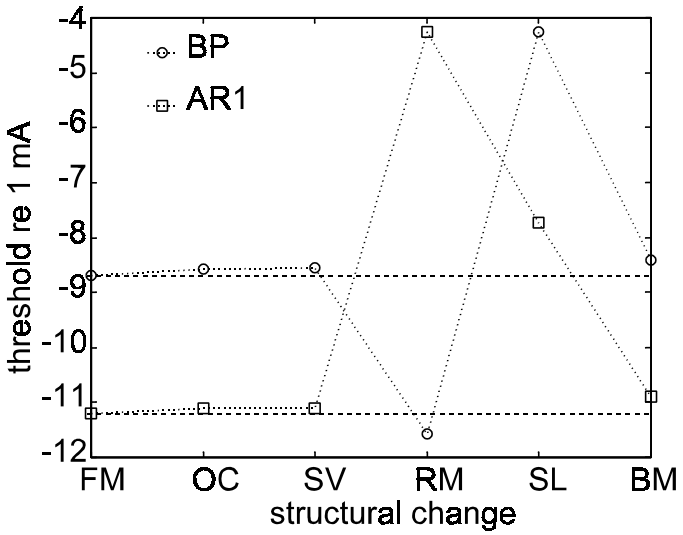

Figure 3.12. Minimum threshold currents as a function of model structure for BP and AR1 electrode configurations for the BM array. FM = full model (no structural changes); OC = Organ of Corti; SV = stria vascularis; RM = Reissner's membrane; SL = spiral lamina; BM = basilar membrane. Dotted lines are added between data points to accentuate differences between threshold currents for the various structural variations.

3.2.2 Electrical tuning curves

Figures 3.13 and 3.14 display spread of excitation as electrical tuning curves. The upper graph in each set shows electrical tuning curves for banded electrode geometries while the lower graph shows electrical tuning curves for point electrode geometries. To enable comparison of electrical tuning curves among different electrode locations and geometries, the minimum threshold current (i.e. the lowest threshold current for any nerve fibre in the model irrespective of stimulus polarity) for each configuration was used as reference (0 dB). Results are again presented for both a full nerve fibre model (solid lines) and a truncated nerve fibre model (dotted lines). Results discussed are for the full nerve fibre model unless stated otherwise. Since electrical tuning curves generated with opposite stimulus polarities differ only marginally, only electrical tuning curves for cathodic-first stimulation on the apical

University of Pretoria etd

electrode are presented.

Electrical tuning curves reach minimum levels on nerve fibres directly opposite the stimulating electrodes for array locations close to the target nerve fibres. Similar to the findings of Frijns (1995) longitudinal displacement of the minima toward the apex relative to the stimulating electrodes often occurs for array locations further away from the nerve fibres. Excitation spread for stimulus intensities below 10 to 30 dB, depending on the electrode configuration, is confined to fibres close to the stimulating electrodes.

3.2.2.1 Bimodal versus unimodal excitation

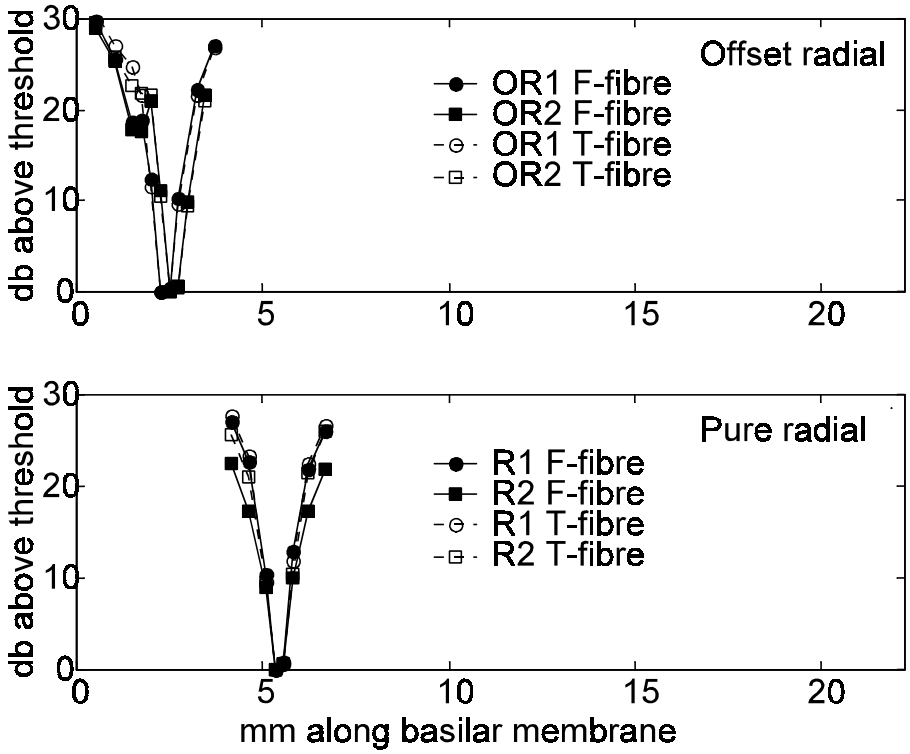

Figure 3.13. Offset radial (upper graph) and pure radial (lower graph) electrode configurations. Electrode locations are not shown.

For bipolar stimulation two regions of excitation, one at each electrode, exist during one stimulus cycle. The magnitude of the central maximum is a function of electrode

University of Pretoria etd

separation. For closely spaced electrode configurations (NBP and BP) the maximum is usually lower than the maximum between more widely spaced electrode configurations. Also, the magnitude of the maximum tends to level off toward wider electrode configurations.

With monopolar (Figure 3.14f) and also with radial and closely spaced offset radial electrode configurations (Figure 3.13) only one threshold minimum occurs, contrary to the two minima created with bipolar longitudinal electrode configurations (Figures 3.14a to 3.14e). For the wider offset radial configuration (OR2), a second region of excitation emerges at approximately 17 dB above threshold. Similar to bipolar configurations, the location of the threshold minimum is independent of polarity. Threshold minima are generally the lowest for radial electrode configurations when the electrode closest to the fibre terminals, i.e. the superior electrode, is used to deliver the cathodic-first stimulus.

3.2.2.2 Spatial selectivity

Most electrical tuning curves for arrays close to the nerve fibres display discontinuities in slope at approximately three model segments (approximately 700 to 820 m along the length of the basilar membrane) from their respective minima. These discontinuities indicate high spatial selectivity close to the electrodes up to stimulus intensities where the discontinuity occurs and less selectivity at stimulus intensities above the discontinuity. The critical focussing intensity (CFI) is defined as the lowest stimulus intensity relative to the minimum threshold at which this discontinuity occurs. The definition specifies the minimum intensity because some variation exists in the exact stimulus intensity where the discontinuity occurs on different sides of the location of a minimum in the electrical tuning curve and also for different electrodes in the array. The CFI gives an indication of the range of relative stimulus intensities over which focussing of neural excitation occurs.

University of Pretoria etd

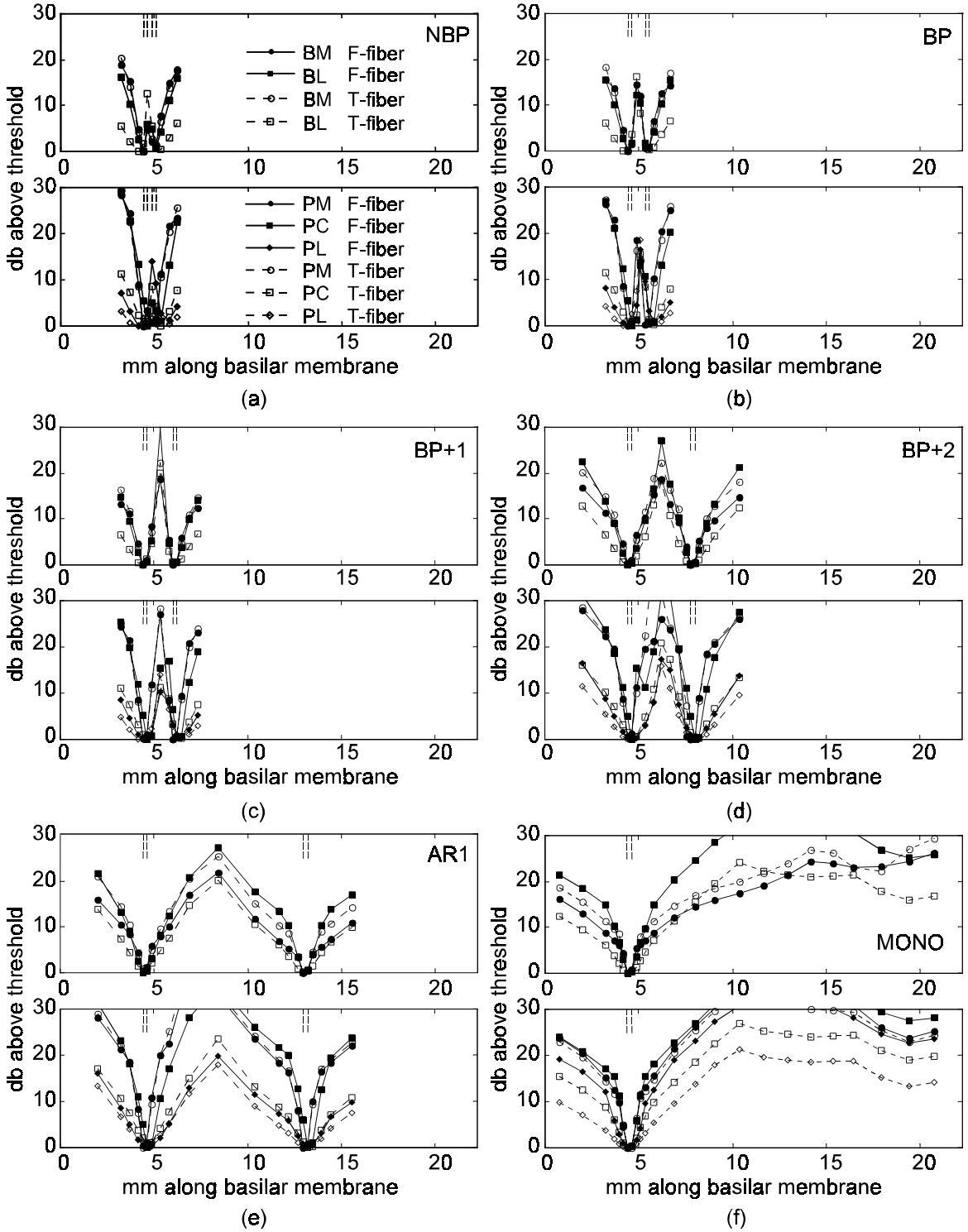

Figure 3.14. Electrical tuning curves for (a) NBP (b) BP, (c) BP+1, (d) BP+3, (e) AR1 and (f) MONO electrode configurations. The legend is shown in (a). "F-fibre" refers to a full nerve model with 16 nodes and "T-fibre" refers to a truncated nerve model with 12 nodes. The location of the electrodes is indicated by the dashed lines in the upper part of each graph.

University of Pretoria etd

The CFI decreases with increasing interelectrode separation (Figure 3.15). For the BM array with a full fibre model relatively localized excitation is achieved up to approximately 15 dB above threshold for NBP electrode configuration, while localized excitation is only achieved up to approximately 4 dB for AR1 electrode configuration. Localized activation is achieved up to approximately 4.4 dB for monopolar stimulation, which is comparable to the localization ability of widely spaced electrode configurations.

The CFI is either not visible or only faintly visible for array locations distal to the nerve fibres, indicating that spread of excitation is more or less directly proportional to interelectrode separation. This is also true for monopolar stimulation if the electrode is located far from the nerve fibres. The CFI is also not very pronounced for radially oriented electrode configurations when compared to those of longitudinal electrode configurations (compare R1 in Figure 3.13 with BM in Figures 3.14a to 3.14e).

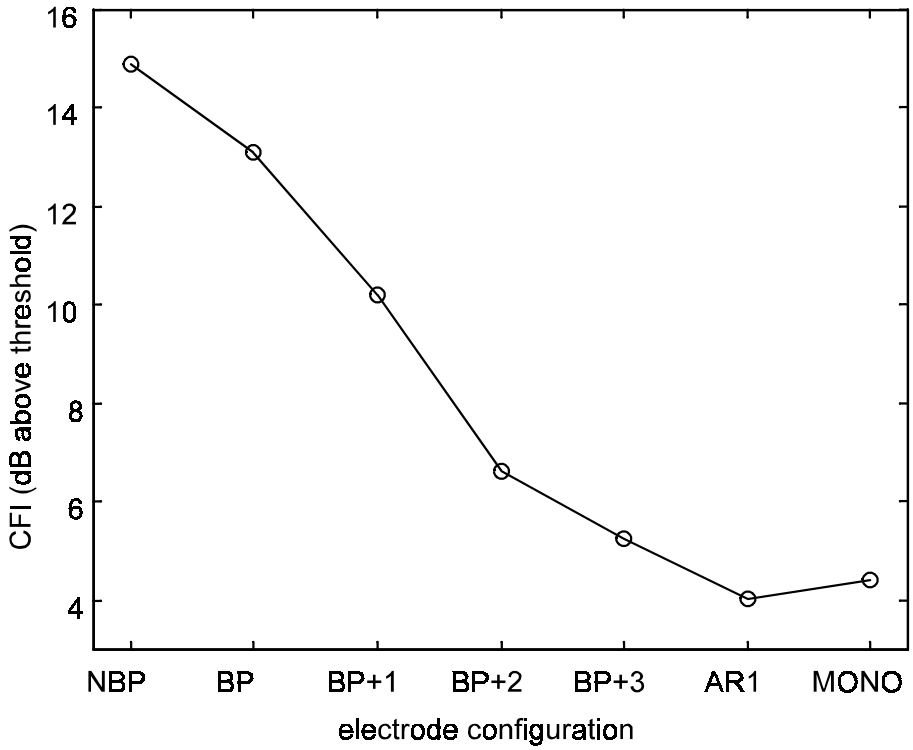

Figure 3.15. CFI as a function of electrode configuration for the BM array for a full nerve fibre model.

University of Pretoria etd

3.2.2.3 Symmetry

The symmetry of excitation around the two electrodes in a longitudinal electrode pair is evaluated by folding electrical tuning curves back onto themselves through a point halfway between the electrodes (Figure 3.16). The effect of unequal model segment lengths is partly compensated for by the mapping of tuning curves onto the same section of the basilar membrane. These plots display a fair amount of symmetry[5] between electrical tuning curves around basal and apical electrodes for closely spaced electrodes. For BP electrode configuration (upper set of graphs in Figure 3.16) substantial deviations from symmetry exist in electrical tuning curves of the PC and PL arrays. Asymmetry is more pronounced for AR1 electrode configuration, shown in the lower set of graphs in Figure 3.16. Though the initial location of excitation along the basilar membrane (i.e. the locations of the minima in the curves) remains unchanged for all array locations except for the PC array (for the full nerve fibre model), excitation is more localized around the basal electrode than around the apical electrode.

3.2.2.4 Spread of excitation

The upper graph in Figure 3.17 shows the spread of excitation close to *one* electrode in an electrode pair along the basilar membrane at 10 dB above threshold for a full nerve fibre model while the lower graph in Figure 3.17 shows the same for a truncated nerve fibre model. Excitation spread for NBP electrode configuration is not included since the regions of excitation for the two electrodes are not separate at 10 dB above threshold. Likewise, results for the PL array for the truncated nerve fibre model are not included above BP+1 electrode configuration since the 10 dB spread exceeds the length of the basilar membrane over which electrical tuning curves were calculated.

---

[5]The term "symmetry" is used to decribe the situation where initial excitation, i.e. minimum threshold current, for both electrodes occur on the same nerve fibre(s), e.g. the BP electrode configuration for the BM array and a full nerve fibre model in the upper set of graphs in Figure 3.16 where the minima occur on the nerve fibres directly opposite the boundaries of the electrodes. Asymmetry is also defined as noticeable differences in the amplitude of the tuning curves.

University of Pretoria etd

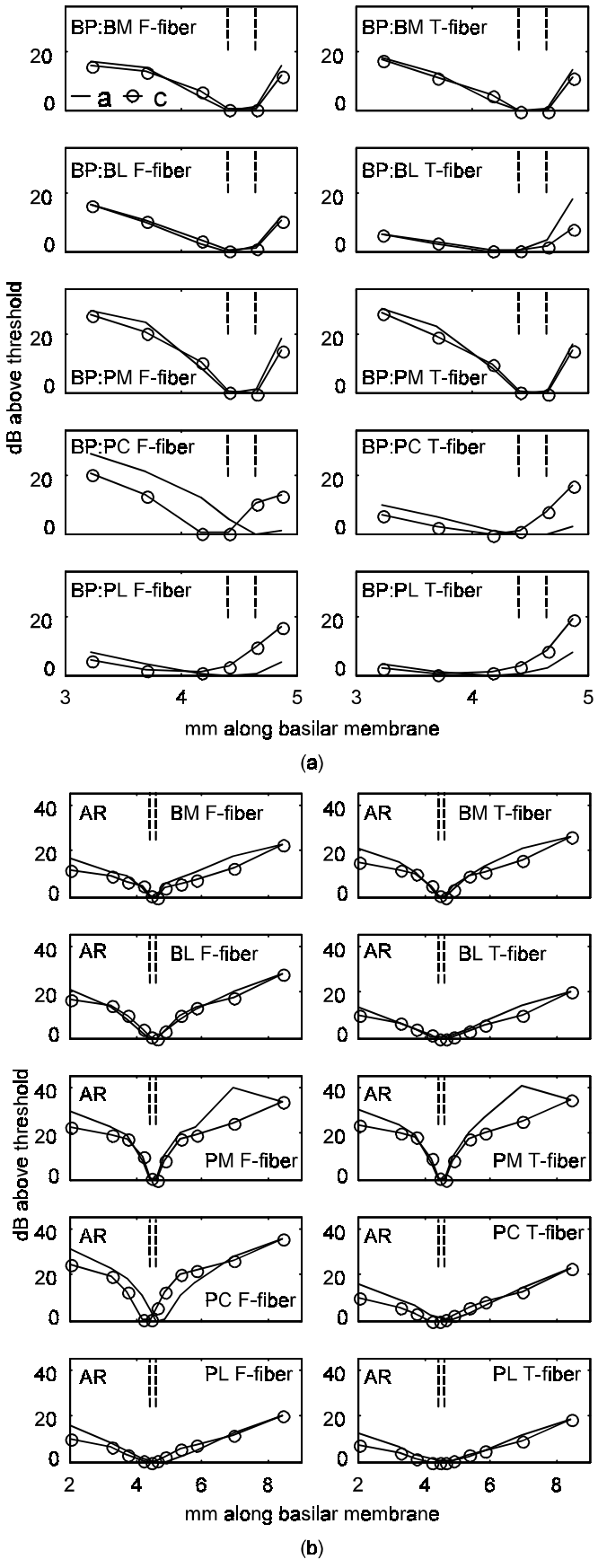

Figure 3.16. Electrical tuning curves of BP (upper set of graphs) and AR1(lower set of graphs) electrode configurations folded back around a point halfway between the electrode contacts to demonstrate the degree of symmetry between excitation pattern generated with the cathodic-first (solid line marked with circles) and the anodic-first (clean solid line) stimuli. Cathodic-first stimuli were applied to the apical electrode, which implies that the left side of the graph would be toward the apex for the cathodic-first curve and toward the base for the anodic-first curve.

University of Pretoria etd

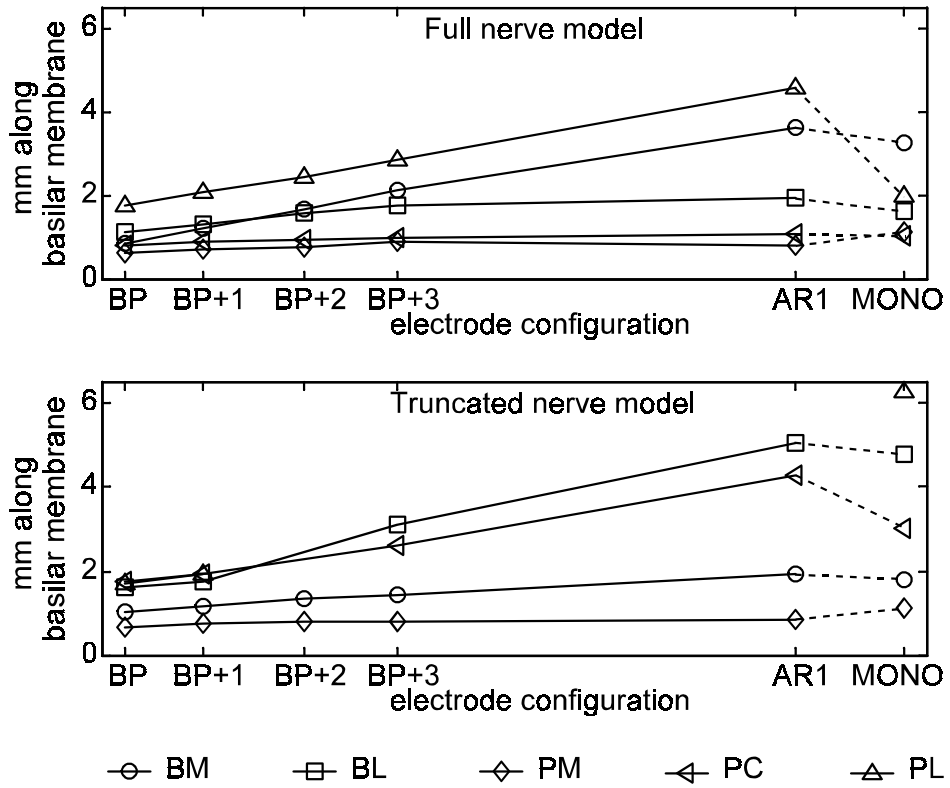

Figure 3.17. Excitation spread along the length of the basilar membrane as a function of electrode separation for a full nerve fibre model (upper graph) and a truncated nerve fibre model (lower graph) at 10 dB above threshold. Note that spread of activation is calculated around *one* electrode only. For bipolar electrode configurations the total spread is approximately twice the values indicated in the figure. Electrode separation for each configuration is indicated to scale relative to BP configuration on the abscissa except for monopolar electrode configuration.

The 10 dB spread levels off for array locations close to the target nerve fibres (except the BM array in the upper graph in Figure 3.17), e.g. for arrays BL, PM and PC when a full nerve fibre model is used and for arrays PM and BM when a truncated nerve fibre model is used. 10 dB spread increases almost linearly with electrode separation for array locations distal to the nerve fibres (and for the BM array when a full nerve fibre model is used). Narrower electrode separations and array locations close to the target nerve fibres usually cause narrower 10 dB spread than widely spaced

University of Pretoria etd

electrode configurations far from the target nerve fibres. For the bipolar electrode configurations the narrowest spread is produced by the PM array under all conditions while the widest spread is produced by the PL array.

For monopolar electrode configuration, spread of excitation is generally lower than for AR1 electrode configuration. It is approximately the same as around one electrode for BP+3 electrode configuration. However, it is interesting to observe that the decrease in spread of excitation relative to that for AR1 is much larger for the PL array using monopolar electrode configuration when a full nerve fibre model is used than for any other electrode geometry or array location. In this case monopolar stimulation yields spread of excitation similar to BP+1 electrode configuration. Like minimum threshold currents, spread of excitation is less sensitive for electrode geometry and array location for monopolar stimulation compared to that for AR1 stimulation.

3.2.2.5 *Ectopic excitation*

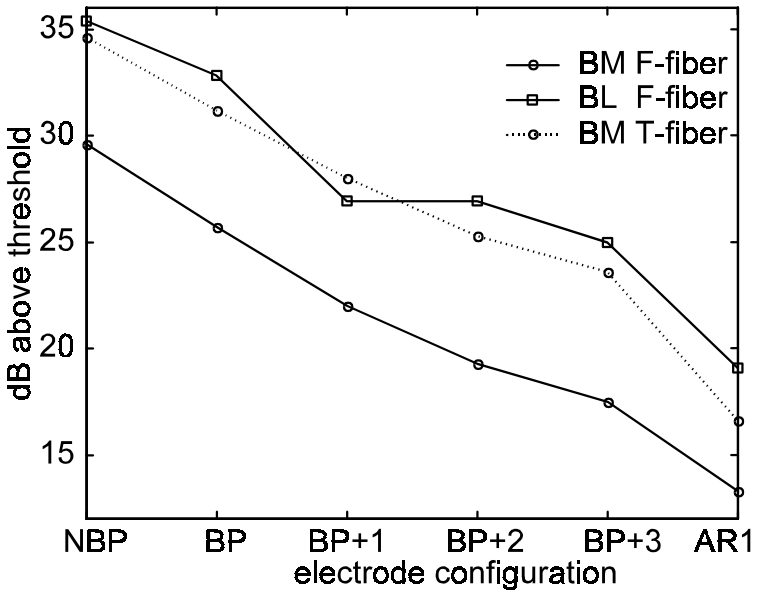

Figure 3.18. Stimulation intensities where ectopic stimulation occurs as a function of electrode separation for different array locations. Legend is explained in the caption of Figure 3.14.

University of Pretoria etd

Ectopic excitation was evaluated by determining threshold currents for nerve fibres originating from the superior cochlear turn. Figure 3.18 shows ectopic stimulation threshold currents for different electrode configurations for the BM and BL arrays using the full nerve fibre model, and also for the BM array using the truncated nerve fibre model. Results show that ectopic stimulation can be expected to occur more readily for widely spaced electrode configurations and that ectopic stimulation for the BM array decreases when the peripheral processes of the nerve fibres have degenerated.

Figure 3.14f shows that for monopolar stimulation, the stimulation current intensity where ectopic stimulation occurs depends on the nerve fibre model used (full or truncated) and the array location. For this case, ectopic stimulation tends to occur at lower stimulation currents when the truncated nerve fibre model is used. The only exception is the BM array for which ectopic excitation occurs at higher stimulus intensities because of the displacement of the fibre terminals relative to the location of the array. The same effect is expected for bipolar electrode configurations.

3.2.2.6 *Resolution of electrode arrays*

Two neighbouring pairs[6] of NBP electrodes (Figure 3.19) have similar excitation patterns with a high degree of overlap. However, an offset (approximately equal to the offset between the electrode pairs along the basilar membrane) exists between the regions of excitation of the two electrode pairs even at high stimulus intensities (10 to 20 dB above threshold).

[6]Two neighbouring pairs in this case are made up of three neigbouring electrodes, i.e. the first pair comprises electrodes *n-1* and *n* and the second pair electrodes *n* and *n+1*.

University of Pretoria etd

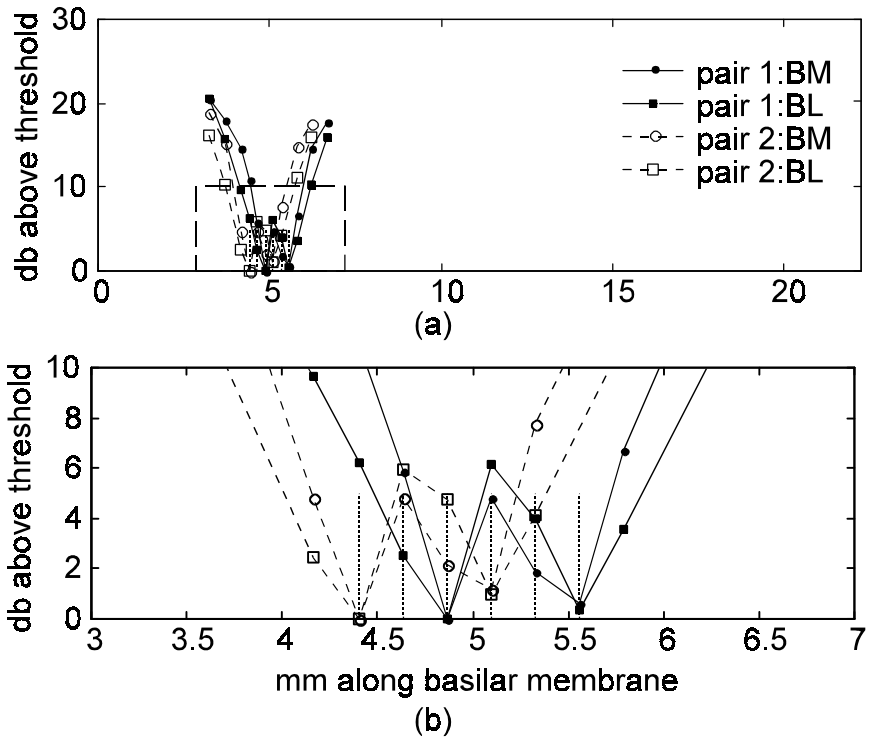

Figure 3.19. Electrical tuning curves generated with two sets of neighbouring NBP electrode pairs (upper graphs). The vertical dotted lines indicate the boundaries of the three electrodes that are used to define the two neighboring electrode pairs (i.e., pair one comprises the left and middle electrodes and pair two the middle and right electrodes). The lower graph shows an enlarged view of the dashed block in the upper graph to present a clear view of the offset between the regions of excitation. Results are for the BM and BL arrays respectively for a full nerve fibre model.

3.2.2.7 Simulated tapering of the scala tympani and scala vestibuli

Scaling of the resistivity of the scalae tympani and vestibuli to simulate tapering of the cochlea does not have a pronounced effect on the spread of excitation at low stimulus intensities (Figure 3.20). However, consistent with what is expected, an increase in spead of excitation at high stimulus intensities can be observed in the tuning curve calculated for the scaled resistivity relative to the tuning curve for constant resistivity closer to the base of the modelled cochlea (upper graph in Figure 3.20) especially for the BM array. The opposite takes place near the apex (lower

University of Pretoria etd

graph in Figure 3.20). Tuning curves calculated at a location halfway through the first half-turn of the cochlea are less affected because the resistivities in this region are approximately equal in both the model with constant resistivity and the model with scaled resistivity.

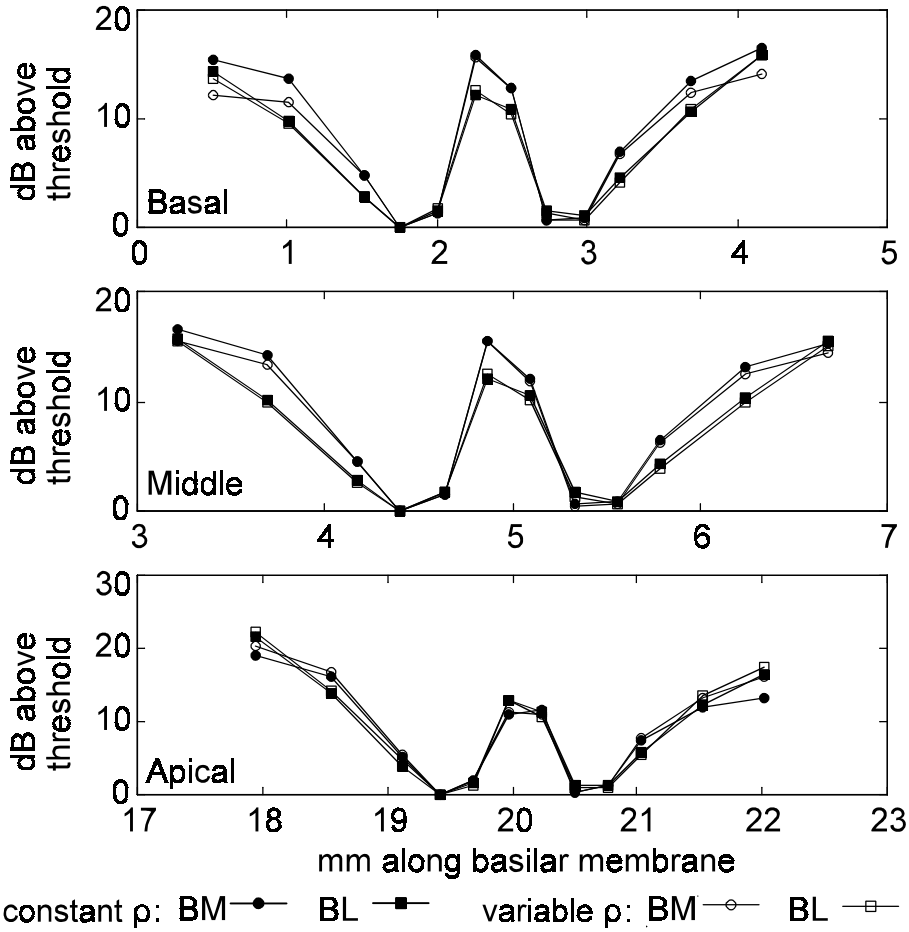

Figure 3.20. Electrical tuning curves at different locations in the modelled cochlea for constant and scaled perilymphatic resistivities. BP electrode configuration was used.

3.2.2.8 Hifocus-like electrode geometries

Electrical tuning curves for the Hifocus-type electrode geometries and for the control electrode geometry are shown in Figure 3.21. Excitation is more localized for the Hifocus-like electrode configurations than for the control geometry for all electrode configurations. The CFI is higher for Hi1 and Hi2 than for the control geometry

University of Pretoria etd

(Figure 3.22). The CFI also tends to be lower for Hi1 than for Hi2, indicating a lower range of stimulus intensities over which focussing occurs.

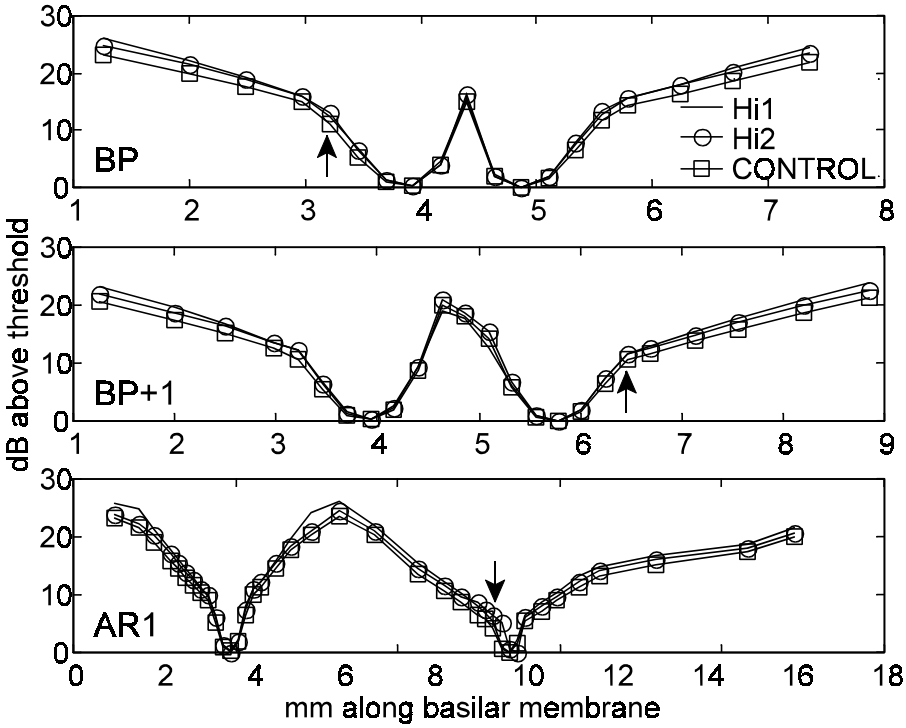

Figure 3.21. Electrical tuning curves for different electrode geometries for BP (upper graph), BP+1 (middle graph) and AR1 (lower graph) electrode configurations. The arrows indicate the location of the CFI in the curves (see Figure 3.23). The legend is the same for the three graphs.

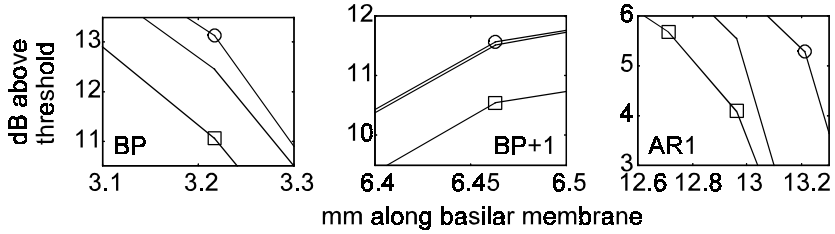

Figure 3.22. An enlarged view of the position of the CFI in Figure 3.21 (arrows) for the electrode geometries Hi1 (no marker), Hi2 (marked with ") and the control geometry (marked with Q).

University of Pretoria etd

The focussing ability of the electrode geometries is calculated as the percentage decrease in spread of excitation along the basilar membrane relative to the control electrode geometry. Both Hi1 and Hi2 exhibits better focussing than the control electrode geometry at all stimulus intensities. For narrowly spaced electrode configurations the focussing ability tends to increase as a function of stimulus intensity. However, there is a limit above which the focussing ability starts to decrease. This limit is clearly visible in the 20 dB curve for AR1 electrode

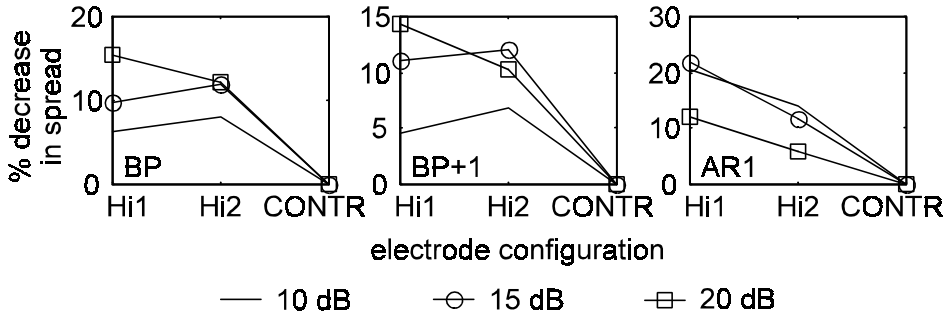

Figure 3.23. Percentage decrease in spread as a function of electrode geometry for BP (left), BP+1 (middle) and AR1 (right) electrode configurations. The legend is the same for the three graphs.

configuration (rightmost graph in Figure 3.23). A decrease in the focussing ability of a test electrode pair relative to a reference electrode pair indicates that the test electrode pair is operating above its CFI or that its focussing ability is less than that of the reference electrode pair. Above their respective CFIs, electrical tuning curves for Hi1 and Hi2 display a constant difference with respect to the tuning curve of the control electrode (i.e. the tuning curves are approximately parallel to one another for AR1 electrode configuration in Figure 3.21). The focussing ability therefore decreases because focussing as a fraction of spread of excitation decreases. For narrowly spaced electrode configurations the focussing ability of Hi1 and Hi2 geometries are similar for 10 and 15 dB relative stimulus intensities. However, at 20 dB relative stimulus intensity Hi1 has better focussing ability than Hi2.

University of Pretoria etd

3.2.2.9 *Influence of cochlear structures on neural excitation*

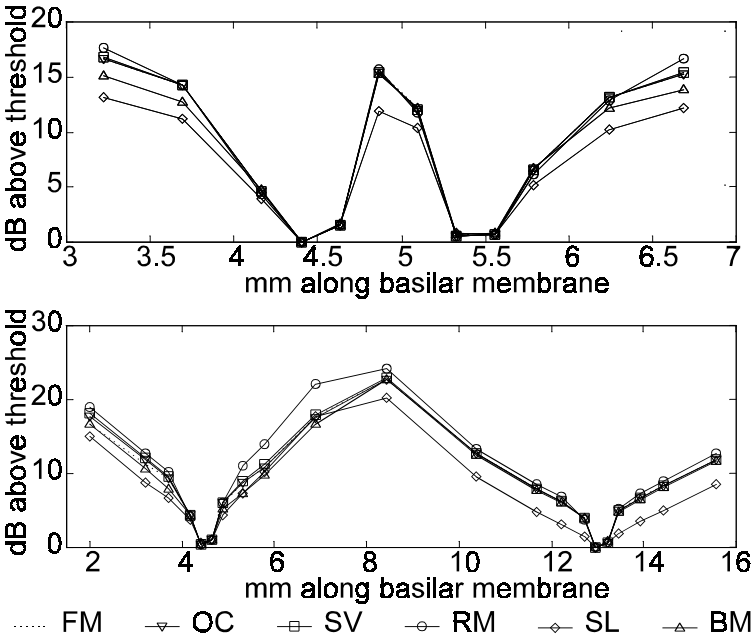

Figure 3.24. Electrical tuning curves showing the effect of omission of the Organ of Corti (OC), stria vascularis (SV), Reissner's membrane (RM), spiral lamina (SL) and the basilar membrane (BM) for BP (upper graph) and AR1 (lower graph) electrode configurations. Results for the full FE model (FM) are also shown.

Inclusion of a helicotrema in the FE model did not have a noticeable effect on neural excitation patterns. Figure 3.24 shows electrical tuning curves as a result of potential distributions generated with structural variations in the FE model for the BM array and BP and AR1 electrode configurations. The basilar membrane and the spiral lamina have the most pronounced influence on excitation patterns. The CFI is lowered in the absence of these structures. This effect is also present, but less obvious for Reissner's membrane. When Reissner's membrane is omitted, spread of excitation is in fact limited relative to spread of excitation in the full FE model for AR1 electrode configuration at stimulus intensities above the CFI. Neither the Organ of Corti nor the stria vascularis has a marked influence on electrical tuning curves.

University of Pretoria etd

4 DISCUSSION

Spread of excitation and minimum threshold currents are both important parameters for the effectiveness and functioning of cochlear implants. Results are thus discussed in terms of these two parameters. Spread of excitation determines the number of independent information channels that can be used to transfer auditory information to the brain. This is because spread of excitation as a result of stimulation with one electrode pair, places a limitation on how close to this electrode pair another pair can be placed to excite a sufficiently different set of nerve fibers so that a sound produced by the first set is discriminable from a sound created by the second set. Spread of excitation therefore has an influence on the number of electrodes that can effectively be used to transfer auditory information (Hanekom & Shannon, 1998).

Threshold currents should be as low as possible for three primary reasons: (1) lower currents are safer for both the electrodes (Rose & Robblee, 1990) and the nerve fibers (Shannon, 1992), (2) consistent use of lower currents prolongs the life of the energy source (Roland et al., 2000; Spelman et al., 1982; Tykocinski et al., 2000) and (3) lower threshold currents could provide an increase in dynamic range (Shepherd et al., 1993).

4.1 Potential distributions and AF contours

The model predicts an increase in the size and intensity of potential distributions for wider electrode separations, consistent with the experimental findings of Suesserman & Spelman (1993), Pfingst et al. (1995) and also with results obtained with the analytical model. Potential distributions generated with the spiralling model are not symmetric for longitudinal electrode configurations. The greatest deviation from symmetry is seen with array locations close to the nerve fibres (e.g. PM in Figure 3.4) and also for widely spaced electrode configurations. Deviations from symmetry for widely spaced electrodes could occur as a result of variation in the length of model segments. However, asymmetry was also observed in some cases for closely

University of Pretoria etd

spaced electrode configurations (e.g. BP electrode configuration for the PC and PL arrays in Figure 3.16a). Asymmetry is thus not only a function of the tapering of the cochlea but also of the spiralling geometry of the cochlea and thus the position of the electrode contacts along the length of the basilar membrane. Asymmetry for BP electrode configuration did not increase noticeably with simulated tapering in the model, probably because the electrode pair was located within segments of constant resistivity (refer to section 2.2.1 of this chapter), e.g. the electrode pairs located at the base and halfway through the first turn of the model, or the electrode pair was situated over a boundary between two resistivities, but the change in resistivity was low, e.g. the electrode pair at the apex of the modelled cochlea. However, in a real cochlea greater asymmetry is expected as a result of tapering of the cochlear canals, especially in the basal region of the cochlea where the diameter of the scala tympani changes rapidly (Hatsushika et al., 1990).

Neural excitation can be evaluated through the activating function (Rattay, 1990; Rattay, 1999) which is proportional to the second spatial derivative of the potential along a long homogeneous nerve fibre. The width of the potential distribution around an electrode gives an indication of the magnitude of the activating function. If the maximum potential is fixed, a wider potential distribution will result in a lower activating function than a narrower potential distribution. Since the activating function at a node is proportional to the nett current flow through the membrane at the node (Finley, Wilson, & White, 1990), the magnitude of the activating function gives an indication of the excitation ability of a potential distribution. A scaled-down version of an activating function (i.e. an activating function with a lower magnitude) will create a narrower region of activation than a scaled-up version of the same activating function. Although this effect is not very profound in the model, it is evident in, for example, the potential distribution for BP+3 electrode configuration for the PM array in Figure 3.4, where the potential distribution around the basal electrode is wider than the potential distribution around the apical electrode. The spread of excitation around the basal electrode at 10 dB above threshold is calculated as 0.72 mm, while the excitation spread around the apical electrode at the same stimulus intensity is

University of Pretoria etd

calculated as 0.92 mm. In the *in vivo* situation the cochlea widens toward the base, which leads to a decrease in the resistance of the volumes close to the electrode contacts (Spelman, Clopton, & Pfingst, 1982). At a specific stimulus intensity one would therefore expect even wider potential spread than predicted with the current model, resulting in narrower spread of excitation. This is consistent with data indicating more localized currents (and thus excitation) around basal electrodes than around apical electrodes (Black, Clark, & Patrick, 1981), as well as increased perceptual thresholds toward the base of the cochlea (Lim, Tong, & Clark, 1989).

Maxima and minima in the AF contours show the location along the basilar membrane (and along the nerve fibres) where excitation can be expected to occur first. The highest activating function intensities occur at the location of the electrodes on the basilar membrane-nerve fibre plane. Maxima and minima occur approximately 0.5 mm from the nerve fibre terminals for medial arrays and at close to the nerve fibre terminals for the lateral array.

AF contours also show that excitation can be expected to spread along the basilar membrane at higher stimulus intensities. This is because the activating function deviates from zero over extended areas along the basilar membrane (Figure 3.4). The intensity of the activating function, which gives an indication of the exciting ability of the stimulus, increases with stimulus intensity, indicating more widespread excitation along the length of the basilar membrane. AF contours also predict an increase in spread of excitation with increasing interelectrode separation. This can be seen in the spatial increase of regions where the intensity of the activating function deviates from zero for wider electrode separations relative to narrower electrode separations. The values of the activating function maxima and minima also increase with interelectrode separation indicating that lower minimum threshold currents are required for widely spaced electrode configurations than for narrowly spaced electrode configurations. This is consistent with the observations of Pfingst et al. (1995).

University of Pretoria etd

4.2 Effects of electrode configuration, electrode geometry and array location

4.2.1 Excitation thresholds

Neural excitation patterns predicted by the model are dependent on the exact location of the electrode contacts relative to the nerve fibre terminals (Kral et al., 1998). In pathological cochleas the distal nerve processes are frequently degenerated (Shepherd, Hatsushika, & Clark, 1993). If degeneration of the peripheral nerve processes is assumed up to the soma, threshold currents change markedly for the BL and PC arrays while remaining relatively unchanged for the PM and BM arrays compared to threshold currents for a full nerve fibre model. Consistent with experimental results from Shepherd, Hatsushika and Clark (1993), much lower threshold currents are predicted for array locations close to the nerve fibres and fibre terminals than for array locations further away. Electrode arrays should thus be placed in close proximity of the modiolus for two reasons: to achieve optimal (i.e. minimum) threshold levels and to reduce the effect of postsurgical neural degeneration (Leake et al., 1992) on threshold currents. Minimum threshold currents are more energy-efficient than high threshold currents and prolong the life of electrodes and the power source of the implant (Roland et al., 2000; Spelman, Clopton, & Pfingst, 1982; Tykocinski et al., 2000).

The use of point electrode geometries is recommended above banded electrode geometries if array location can be controlled. However, banded electrode geometries are superior to point electrode geometries for obtaining low threshold currents when the array location cannot be precisely controlled, as is evident from high threshold currents obtained with the PL array (Figure 3.8e) and also the PC array (Figure 3.8d) when a truncated nerve fibre model is used.

Minimum threshold currents determined for Hifocus-like electrode geometries are lowest when the electrodes are recessed into the electrode carrier on all sides (Hi1). Partly recessed electrodes (insulating pillows between the contacts) also lower minimum threshold currents relative to non-recessed electrodes, but not as much as totally recessed electrodes. The planar nature (Advanced Bionics Corporation, 8-21-

University of Pretoria etd

2000) of the electrodes of the Hifocus electrode, which could also limit current spread, was not modelled (the modelled electrode approximates a curved surface). However, based on model results for a curved electrode surface, the focussing ability of the Clarion Hifocus electrode could potentially be improved further by extending the electrode carrier over the superior and inferior sides of the contacts so that these sides are also recessed like the lateral sides.

Several researchers have presented data showing that initial excitation can be produced by either the anodic or cathodic phase of a stimulus waveform (Liang, Lusted, & White, 1999; van den Honert & Stypulkowski, 1987). Also, the polarity of the leading phase in a biphasic stimulus does not have a pronounced influence on the minimum current required to elicit a nerve fibre response. When the electrode contacts are close to the fibre terminals or distally toward the outer wall of the scala tympani, the nerve fibre model usually predicts lower threshold currents for nerve fibres close to the basal electrode than for nerve fibres close to the apical electrode in an electrode pair, irrespective of stimulus polarity. However, as a consequence of the manner in which the model was constructed (equal angle sections), lower thresholds would be expected for the apical electrode (smaller surface area and thus higher current density) if only the electrode surface area and its proximity to the nerve fibres were to determine minimum threshold currents. Model results therefore suggest that the location of the electrodes along the length of the basilar membrane has a stronger influence on the location of excitation along the basilar membrane than the polarity of the stimulus waveform. This observation cannot be fully tested with the current model since the equal angle model segments cause variation in the surface area of electrode contacts. The model does not allow continuous tapering of the cochlea either. Models incorporating tapering of the cochlea and constant electrode surface areas, and also measurement of neural excitation in the vicinity of both electrodes in an electrode pair in real cochleas, are required to verify the observation.

University of Pretoria etd

4.2.2 Spread of excitation

The CFI of a specific electrode pair gives an indication of the dynamic range over which relative focussed stimulation can be expected for that electrode pair. Variations in the CFI can be expected between different pairs of the same electrode configuration since it could be affected by electrode to nerve fibre proximity, the impedance pathway between the electrodes, electrode geometry and survival patterns of auditory nerve fibres. EABR input-output functions measured by Shepherd, Hatsushika and Clark (1993) on cats display a CFI in most cases. For electrodes placed near the spiral ganglion and the dendrites, the CFI is between 16 and 20 dB above threshold for BP electrode configuration and between 3.5 and 14 dB above threshold for BP+1 and BP+2 electrode configurations.

Five observations can be made from the CFI for different electrode configurations: 1) closely spaced bipolar electrode configurations have the best focussing ability, 2) if focussing is desired, an electrode pair should ideally operate at stimulus intensities below its CFI, 3) for electrode configurations that do not show a CFI, there is no critical range of operation, i.e. spread of excitation is proportional to stimulus intensity, 4) the focussing ability of monopolar electrode configurations is comparable to that of widely spaced bipolar electrode configurations, and 5) the focussing ability of recessed electrodes is higher than that of unrecessed electrodes.

Three observations regarding the effect of electrode configuration and array location on excitation patterns can be made from 10 dB excitation spread and will be explained below: 1) electrode separation cannot compensate for array location, 2) there is little difference between BP, BP+1, BP+2 and BP+3 electrode configurations, 3) excitation spread generated by array locations distal from the target nerve fibres increases significantly at wide electrode separations. Implications for cochlear implant subjects are the following: If threshold cannot be achieved with narrowly spaced electrode configurations, more widely spaced configurations (up to BP+3) can be used without a considerable increase in the 10 dB spread. This is also evident from

University of Pretoria etd

gap threshold data[7] (that give an indication of the amount of interaction between electrodes) that are similar for BP to BP+3 electrode configurations (Hanekom & Shannon, 1998) and from pitch ranking experiments where subjects' performances were similar for BP+1 and BP+3 electrode configurations (Hanekom & Shannon, 1996). The most effective way to control excitation spread is thus by controlling the location of the array relative to the target nerve fibres, i.e. arrays close to the target nerve fibres create more localized excitation spread. Electrode separation can to a limited extent be used to control excitation spread (i.e. closely spaced electrode configurations limit excitation spread) but not as effectively as correct placement of the array. When an array is located toward the outer wall of the scala tympani, as is often the case with the Nucleus implant (Shepherd, Hatsushika, & Clark, 1993), closely spaced electrode configurations should be used to limit spread of excitation. Again, a banded electrode geometry is superior to a point electrode geometry to limit excitation spread in this case (compare results for arrays BL and PL in Figure 3.17). Results for the AR1 configuration suggest that excitation (at comfortable stimulus intensities) is less localized with arrays located far from the target nerve fibres and is similarly not localized with true monopolar stimulation if the array is far from the target nerve fibres. However, localization is possible with AR1 and also with true monopolar stimulation when the array is close to the modiolus.

Based on the CFI and spread of excitation as functions of electrode configuration,

[7]Gap threshold is the minimum duration of a temporal gap between two sounds (i.e., sound, silence, sound) that is detectable by the auditory system. For cochlear implant wearers the experiment is performed by applying two stimuli to either the same electrode set or different electrode sets before and after a non-stimulation period. Hanekom and Shannon (1998) used two different sets of electrodes to deliver the stimuli. For this case, gap detection is presumably determined by a centrally located auditory integration mechanism. The more distinct the two excited neural populations, the longer the integration time constant and the higher the gap threshold. Similar gap thresholds for BP to BP+3 electrode configurations imply that the excited neural populations are similar and are therefore caused by similar spreads of excitation.

University of Pretoria etd

monopolar stimulation is recommended above widely spaced bipolar stimulation because of three reasons. Firstly, because focussing ability for the two configuration types is comparable, secondly because the unimodal excitation pattern of monopolar stimulation implies that only the intended neural population is activated and thirdly, because spread of excitation for monopolar stimulation is in actual fact approximately half that of widely spaced electrode configurations.

4.2.3 Banded versus point electrode geometries

A general overview of simulation results indicates that point electrode geometries and banded electrode geometries behave differently when they are located close to the fibre terminals. In general, a point electrode array close to the fibre terminals produces excitation paterns similar to those produced by an array overlapping with the nerve fibres, i.e. its behaviour is similar to that of the BM and PM arrays, while a banded electrode array at the same location produces excitation patterns similar to those produced by a laterally located array, i.e. its behaviour is similar to those of the BL and PL arrays.

4.3 Ectopic stimulation

Ectopic stimulation was evaluated by determining the stimulus intensity above threshold where *modelled* nerve fibres from the superior cochlear turn will be excited. Nerve fibres located in the region between the target nerve fibres and nerve fibres from superior cochlear turns will be excited at stimulus intensities between threshold currents for these two nerve populations. Also, the cochlea in the model is 25% higher than a real cochlea, which causes an underestimation of ectopic stimulation as a result of current spread to neighbouring cochlear canals. Figure 3.18 thus gives a relative indication of the occurrence of ectopic stimulation that can be expected with a specific electrode configuration and array location. Excitation spreads along the cochlear canal rather than across the modiolus or across neighbouring canals, i.e. excitation of nerves from superior cochlear turns occurs only at higher stimulus intensities. Ectopic stimulation occurs more readily for widely spaced electrode configurations than for closely spaced electrode configurations. Similarly, medial

University of Pretoria etd

array locations are more prone to ectopic excitation than arrays located more distally relative to the nerve fibres. There is thus a tradeoff between the extent of ectopic excitation and the proximity of the array to the target nerve fibres, especially at wider electrode configurations. The optimal arrangement to reduce ectopic excitation would thus be a *laterally* located array using a *closely spaced* electrode configuration. However, to reduce the spread of excitation along the length of the basilar membrane and to limit threshold currents, medial array locations are preferable, making the use of narrowly spaced electrode pairs even more important. Ectopic excitation can, however, also be defined as any unintentionally stimulated nerve fibres. According to this definition, one of the minima in the bimodal excitation pattern generated by bipolar electrode configurations is also an ectopic excitation region.

4.4 Bimodal versus unimodal excitation patterns

Anodic-first to cathodic-first threshold ratios for charge-balanced biphasic stimulation are close to unity in most cases, implying a very small difference in the excitation ability of the two electrodes in an electrode pair. At comfortable stimulus intensities[8] of 4.5 to 22.5 dB above threshold, bimodal excitation exists when a bipolar electrode configuration is used. These two excitation regions have been modelled (Frijns, 1995; Kral et al., 1998) and measured (Kral et al., 1998) for longitudinal bipolar stimulation. Eddington et al. (1988) also reported that subjects describe sound sensations generated with bipolar electrodes as "not as pure" as sensations generated with monopolar electrode configurations. To create a single region of excitation one of four electrode configurations can be used: NBP, offset radial, radial and monopolar electrode configurations. The two regions of excitation around the electrodes in an NBP electrode configuration overlap to a great extent if the array is located close to the nerve fibres, creating a single region of excitation above approximately 5 dB above threshold. However, excitation threshold currents for NBP are high compared to other electrode configurations (Figure 3.8).

[8]Comfortable stimulus intensities are assumed to be at 75% of dynamic range, which is 6 to 30 dB (Shannon, 1983).

University of Pretoria etd

Offset radial and pure radial electrode configurations are optimal for creating a single region of excitation at all stimulus intensities (Figure 3.13). Threshold currents are much lower for radially oriented configurations (up to 17 dB) than for NBP configurations and also (to a lesser extent) for monopolar electrode configurations. Threshold differences between NBP for the PM array and the radially oriented configurations are, however, not significant. However, NBP configuration creates a wider region of excitation under all circumstances than radially oriented configurations (compare Figures 3.13 and 3.14a). Thus, NBP configuration would only be advantageous if a banded electrode geometry is used. If a point electrode geometry is used, radially oriented electrode configurations are the configurations of choice because of their lower threshold currents and narrower regions of excitation. Offset radial electrodes should, however, not be separated by more than approximately 1 mm where a second region of excitation emerges at stimulus intensities in the order of 17 dB above threshold.

4.5 Resolution of intracochlear electrode arrays

Although excitation is not necessarily localized at higher stimulus intensities, model results indicate that excitation regions are different for different electrodes even when the electrodes in a bipolar pair are narrowly spaced (NBP). Based on this observation, the resolution of cochlear implant electrodes could potentially be improved, which could lead to improved speech recognition (Kral et al., 1998). The model firstly suggests that localized excitation is possible with NBP electrode configuration although threshold currents are 2 to 3 dB higher than threshold currents for BP electrode configuration (Figure 3.8). Secondly, results suggest that excitation profiles created with two bipolar pairs made up from three adjacent closely spaced electrodes are *different* since the regions of excitation do not overlap completely. It is possible that cochlear implant subjects can discriminate between overlapping though different excited nerve populations (Liang, Lusted, & White, 1999; Pfingst et al., 1999). Evidence of this is found in electrode discrimination data where subjects could rank pitch consistently for a number of neighbouring, overlapping electrode pairs using BP+1 and BP+3 electrode configurations (Hanekom & Shannon, 1996).

University of Pretoria etd

NBP electrode configuration close to the surviving nerve fibres could limit threshold currents to values for which the full dynamic range of the nerve population can be included within the range of currents deliverable with the prosthesis. However, for arrays located toward the outer wall of the scala tympani threshold currents might exceed the stimulator's maximum current. Still, a greater number of electrodes could be beneficial if wider electrode separations are used. The current model contains 45 closely spaced electrode contacts that could provide 43 BP longitudinal electrode pairs which could potentially activate 43 different (but overlapping) sets of nerve fibres. Less overlap between excited nerve populations will occur if *radially* oriented electrode configurations are used. With well-placed arrays, e.g. the Clarion electrode array (Kessler, 1999), it might be possible to create at least two significantly different regions of excitation per mm along the length of the basilar membrane. An electrode array with a penetration depth of 25 mm could thus potentially create 50 different regions of excitation. This finding is supported by experimental data from Jolly et al. (1997) that show that a high contact density electrode array, i.e., an electrode array with center-to-center contact separation of 225 m, can effect excitation of nerve fibers if it is placed close to the spiral ganglion cells.

4.6 Variations in the cochlear model

Model results supplied a qualitative measure of the importance of different cochlear structures with respect to modelling. Inclusion of the helicotrema in the FE model did not have a significant effect on potential distributions and consequently on threshold currents and neural activation patterns. Exclusion of the Organ of Corti and the stria vascularis did not have an adverse effect on model results. The spiral lamina, Reissner's membrane and the basilar membrane do, however, play an important role during calculation of threshold currents and also spread of excitation. Future FE models could thus be constructed without the helicotrema, Organ of Corti and the stria vascularis, but have to include the spiral lamina, Reissner's membrane and the basilar membrane.

Tapering of the cochlea as simulated by scaling of the resistivity of the perilymphatic

University of Pretoria etd

spaces has a significant effect on primarily threshold currents for stimulation at different locations in the cochlea. Lower threshold currents at the base of the cochlea relative to threshold currents at a more apical location in the cochlea have been experimentally observed in implant users (Ulehlova, Voldrich, & Janisch, 1987). This is associated with a more proximal location of the array relative to the nerve fibres towards the apex because of tapering of the cochlea. In addition, model results suggest that an electrode at the same distance from the target nerve fibres will display different threshold currents at different locations in the cochlea because of the variation in resistance of the volume conductor that results from tapering of the cochlea. The effect of scaled resistivity on excitation patterns is less prominent, but present in the model. Spread of excitation tends to increase at the base of the cochlea where the resistance of the volume conductor is lower relative to the resistance towards the apex[9], especially at higher stimulus intensities. In this thesis most simulations were performed in a specific region of the cochlea. For these simulations the effect of tapering of the cochlea is thus negledible. However, it is concluded that tapering of the cochlea is an important model parameter when an extended region of the implanted cochlea is modelled.

5 CONCLUSIONS

The following observations were made from this study:

1) Asymmetry in potential distributions is not only a function of the tapering of the cochlea but also of the spiralling geometry of the cochlea. Also, the location of electrodes along the length of the basilar membrane has a stronger influence on the location of excitation along the length of the basilar membrane than the polarity of the leading phase of the stimulus waveform.

[9]Note, however, that at a specific stimulus intensity, spread of excitation is lower for electrodes located towards the base than for electrodes towards the apex because the minimum threshold current required to elicit a response is higher for basally located electrodes. Refer to page 83.

University of Pretoria etd

2) The helicotrema, stria vascularis and Organ of Corti do not have a significant effect on potential distributions, minimum threshold currents and neural excitation patterns in the model presented. Inclusion of the spiral lamina, Reissner's membrane and the basilar membrane in 3-D models of the implanted cochlea is required to obtain accurate estimates of potential distributions.

3) To limit threshold currents and to limit the effect of postsurgical neural degeneration on threshold currents, arrays should be placed close to the modiolus. Point electrode geometries are recommended above banded electrode geometries only when the array can be placed close to the modiolus.

4) When close to the fibre terminals, point electrode arrays produce excitation patterns similar to those produced by arrays close to the nerve fibres, while banded electrode arrays produce excitation patterns similar to those produced by arrays far from the target nerve fibres.

5) Array location is the primary parameter that controls excitation spread. A secondary but less effective parameter is electrode separation. Consequently, there is little difference in excitation spread generated with BP, BP+1, BP+2 and BP+3 electrode configurations. Excitation spread for array locations distal from the target nerve fibres increases notably for wide electrode separations.

6) There is a tradeoff between the proximity of the array to the target nerve fibres and the degree of ectopic excitation caused by the specific array location. Laterally located arrays using closely spaced electrode configurations limit ectopic excitation most efficiently. However, if an array is placed close to the nerve fibres to reduce threshold currents and spread of excitation, closely spaced electrode pairs should be used to limit ectopic excitation.

7) Bimodal excitation exists at comfortable stimulus intensities for longitudinal bipolar electrode configurations. Radial and monopolar electrode configurations are optimal to create unimodal excitation. NBP electodes can alternatively be used to create unimodal excitation for longitudinal electrode configurations, but have higher threshold currents and broader excitation

University of Pretoria etd

regions than radial electrode configurations.

8) The focussing ability of monopolar electrode configurations is comparable to that of widely spaced bipolar electrode configurations. In addition, spread of excitation is limited with monopolar stimulation relative to that of widely spaced bipolar stimulation. In contrast to bipolar electrode configurations, only the target nerve fibres are activated during monopolar stimulation because of the unimodal excitation pattern resulting from monopolar stimulation.

9) The resolution of cochlear implant electrode arrays can potentially be improved to at least two different locations of excitation per mm along the basilar membrane if arrays are placed close to the modiolus.